[AMERICAN JOURNAL OF SCIENCE, VOL. 289, MARCH, 1989, P. 217–248]

American Journal of Science

MARCH 1989

LIQUID-VAPOR RELATIONS FOR THE SYSTEM NACl–H_2O: SUMMARY OF THE P-T-x SURFACE FROM 300° TO 500°C

JAMES L. BISCHOFF* and KENNETH S. PITZER**

ABSTRACT. Experimental data on the vapor-liquid equilibrium relations for the system NaCl–H_2O were compiled and compared in order to provide an improved estimate of the P-T-x surface between 300° to 500°C, a range for which the system changes from subcritical to critical behavior. Data for the three-phase curve (halite + liquid + vapor) and the NaCl–H_2O critical curve were evaluated, and the best fits for these extrema then were used to guide selection of best fit for isothermal plots for the vapor-liquid region in-between. Smoothing was carried out in an iterative procedure by replotting the best-fit data as isobars and then as isopleths, until an internally consistent set of data was obtained. The results are presented in table form that will have application to theoretical modelling and to the understanding of two-phase behavior in saline geothermal systems.

INTRODUCTION

Much attention is focused on the system NaCl–H_2O because of its fundamental importance to the understanding of electrolyte behavior and for its importance in many geological processes. NaCl is the primary solution in most hydrothermal and metasomatic fluids. The two-phase region of this system has become of particular interest because of the recently accumulating evidence that phase-separation is an important process in many hydrothermal systems and, in particular, seafloor geothermal systems (for example, Bischoff and Pitzer, 1985; Delaney, Mogk, and Mottl, 1987; Fournier, 1987). Seawater circulates in these systems between the seafloor and the tops of subsurface magma chambers, with hydrostatic pressures ranging from approx 100 to 600 bars. These pressures bracket the P-T two-phase univariant curve for seawater (3.2 wt percent NaCl) for the temperatures from 300° to 500°C.

The two-phase region of NaCl–H_2O is extremely large and occupies a significant portion of the P-T space to which circulation in the seafloor systems is constrained. Because molten magma at temperatures in excess of 800°C is episodically injected at depth into seawater-saturated permeable rocks in these systems, circulating seawater must on occasion be thrust into the two-phase region (Fournier, 1987).

* U.S. Geological Survey, Menlo Park, California 94025
** Department of Chemistry and Lawrence Laboratory University of California, Berkeley, California 94720

The two-phase region of NaCl–H_2O undergoes a rather complex geometric change from below the critical point of pure water to above, and the properties of the system change dramatically. Accurate theoretical modeling of this rather complex part of the system is a particular challenge, and its successful execution will serve as a model for other ionic salts. Thus, an accurate portrayal of the pressure–temperature–composition (P-T-x) relations of the two-phase surface, particularly for the range of conditions of the present study, is an important basis for the formulation of theoretical models. A theoretical model for halite-saturated vapor has been presented by Pitzer and Pabalan (1986), for the single-phase liquid region of NaCl–H_2O by Pitzer and Li (1984) and Pitzer, Peiper, and Busey (1984), and for the critical region by Pitzer, Bischoff, and Rosenbauer (1987). Tanger and Pitzer (in press) have expanded the latter work to model the two-phase region from the critical region down to halite-saturation and achieved approximate agreement with experimental data for 250° to 600°C.

The most extensive experimental work on the vapor-liquid relations of the system NaCl–H_2O is that of Sourirajan and Kennedy (1962) who carried out experiments from 350° to 700°C. In addition there are a number of studies (for example, Ölander and Liander, 1950; Khaibullin and Borisov, 1966; Urosova, 1974, 1975) that provide data over less extensive ranges of conditions. The data from many of these studies are at variance with those of Sourirajan and Kennedy for some conditions. Compilation and comparison of the various studies were deemed necessary to determine the best estimate of the two-phase surface in P–T–x space.

When we began the compilation of the experimental studies on the two-phase surface from the literature for the range 300° to 500°C, it became evident that there were important P-T conditions for which little or no experimental data existed and other conditions where considerable scatter existed, and there was no basis for selection. Thus, a series of experimental studies were carried out to fill in these gaps (Bischoff, Rosenbauer, and Pitzer, 1986; Rosenbauer and Bischoff, 1987; Pitzer, Bischoff, and Rosenbauer, 1987; and Bischoff and Rosenbauer, 1988).

With the completion of these studies the data set is considered sufficiently complete to justify the summary that follows. The objective was to prepare a table of P–T–x points on the two-phase surface that reflects the present state of knowledge.

TOPOLOGY OF THE TWO-PHASE SURFACE

NaCl–H_2O is a binary system in which the solubility of halite in the vapor is considerable and in which the solubility curve of halite in coexisting vapor and liquid does not intersect the critical curve in P-T projection (Morey, 1957). Vapor-liquid relations in this sytem, as in any two-component system, are represented by a P–T–x surface. For the full range of conditions, the relations are shown diagrammatically in sepa-

rate two-dimensional projections in figure 1A, B, and C as modified and expanded after Morey (1957), Bodnar, Burnham, and Sterner (1985), Pitzer and Pabalan (1986), and Fournier (1987). An oblique view of that part of the surface that corresponds to the 300° to 500°C range of the present study is shown in figure 2. In P-T projection of the full range of conditions (fig. 1A) the one-component diagram for pure H_2O is shown on the left side of the diagram, and the corresponding diagram for pure NaCl on the right. These two parts of the diagram are on different planes of the composition axis, with the pure H_2O diagram on the forward face of figure 1A and NaCl diagram on the back face. The vapor-liquid region extends to a very large field between these two faces. This field is bounded at low pressures by halite solubility in coexisting liquid and vapor (three-phase assemblage) which extends from the invariant point (P) of the assemblage hydrohalite–halite–liquid–vapor at 0.1°C and 0.005 bar (which is immediately above the invariant eutectic, point E, of the assemblage halite–ice–liquid–vapor at −20.8°C and 0.001 bar) to a maximum pressure of 392 bars at 600°C after which the pressure decreases with increasing temperature until the triple point of NaCl marked by TP (NaCl) at 801°C and 3×10^{-4} bar is reached (Chase and others, 1985; Linke, 1965). The sharp drop in pressure as temperature increases from 600° to 800°C is a consequence of the decreasing fraction of H_2O relative to NaCl in the liquid and vapor phases, as the pure NaCl end point is approached. At high pressures the two-phase region is bounded by the boiling curve at H_2O extending from the triple point of water, TP(H_2O), to its critical point (CP H_2O) at 374°C, 220 bars, and its approximately co-linear extensions as the NaCl–H_2O critical curve which terminates at the NaCl critical point estimated to be 3600°C, 260 bars, after going through a maximum estimated to be at 2000°C, 2500 bars (Pitzer, 1984). Where the ratio of the critical temperature of the two components is large, as it is for NaCl–H_2O, some systems show liquid-liquid phase separation over a temperature range near the lower of the critical temperatures (Rowlinson and Swinton, 1982); examples include CH_4 with n-hexane or n-heptane. The aqueous system UO_2SO_4–H_2O also shows liquid-liquid immiscibility beginning at 286°C and 70 bars (Marshall and Gill, 1974). The system NaCl–H_2O has been adequately investigated throughout the corresponding range of temperature, however, and shows no liquid-liquid immiscibility: hence the evidence strongly supports the simple phase diagram with the single critical line extending from the critical point of H_2O to that of NaCl as shown in figure 1A. Also shown in figure 1A are isopleths of wt percent NaCl with liquid limbs extending from lower temperature to the respective critical points and the vapor limbs extending in sweeping curves from the critical points to immediately above the triple-point of NaCl. The points of maximum pressure on the vapor limbs have been termed "hypocritical points" by Fournier (1987). An isopleth for 3.2 wt percent NaCl would represent the complete P-T boundary for seawater, with the liquid limb up to the critical point representing the boiling

curve and the vapor limb the condensation curve. For reference, an isopleth of halite solubility in single-phase liquid (50 wt percent NaCl) and that in single-phase vapor (0.015 wt percent NaCl) are shown. These isopleths meet at a point on the curve of the three-phase assemblage where they are in equilibrium.

In T-x projection (fig. 1B) the same elements are seen. In this case, the three-phase assemblage is represented by separate curves for the liquids and vapors extending from their respective invariant compositions (P_V, P_L and E_V, E_L) to the triple-point of NaCl. Horizontal tie-lines between these two curves represent the composition of coexisting liquids and vapors in equilibrium with halite. The three-phase vapor curve shows a continuous increase in wt percent NaCl to about 550°C above which the trend reverses to very low concentrations as just below 800°C where the curve abruptly reverses to approach 100 wt percent at NaCl triple-point. The shape of this curve is predicted by the theoretical model of Pitzer and Pabalan (1986) and differs significantly from earlier visualizations (for example, fig. 19 of Sourirajan and Kennedy, 1962). For reference, three isobars describing coexisting vapors and liquids within the two-phase region are shown, two of which are within the range of pressures of the present study. Isobars below the critical pressure of water, represented by 200 bars, are characterized by a liquid and vapor limb extending from the three-phase assemblage and meeting at the boiling temperature of water (at 0 wt percent NaCl) in a beak-like projection. Above the critical pressure of water the pattern is considerably changed. Isobars from 220 to 392 bars (from the critical pressure of pure water to the maximum pressure on the halite–liquid–vapor curve) are U-shaped with limbs extending from separate liquid and vapor points on the halite–liquid–vapor curve and meeting at the critical point on the NaCl–H_2O critical line as illustrated by 350 bars. Above 392 bars, the isobars are tear-shaped with limbs extending from a single point in the supercritical region of pure NaCl and meeting at a critical point on the NaCl–H_2O critical line, as illustrated by 750 bars. Horizontal tie-lines on each isobar represent the compositions of coexisting vapor-liquid pairs at various temperatures. In P-x projection (fig. 1C) the

Fig. 1. Schematic P-T-x relations for the vapor-liquid region of the system NaCl-H_2O, modified and expanded after Morey (1957), Bodner, Burnham, and Spencer (1985), Pitzer and Pabalan (1986), and Fournier (1987). TP(H_2O) and TP(NaCl) are the melting points (triple points) of pure H_2O and NaCl, respectively. CP(H_2O) and CP(NaCl) are the critical points of pure H_2O and NaCl, respectively. E is the NaCl–H_2O eutectic (hydrohalite-ice-liquid-vapor, E_L and E_V refer to the eutectic liquid and eutectic vapor compositions, respectively), and P is the invariant point of the assemblage halite-hydrohalite-liquid-vapor (P_L and P_V refer to the liquid and vapor compositions respectively).

(A) P-T projection showing isopleths of wt percent NaCl in the vapor-liquid region (red lines). Vapor limbs of isopleths (solid red) extend from critical points to immediately below the melting point of NaCl. Liquid limbs (dashed red) extend from either the melting curve of ice or from the three-phase curve (halite + vapor + liquid) to the critical points. The dashed black line shows the 50 wt percent isopleth of halite solubility in single-phase liquid, and the dotted lines show the 0.1 and 0.015 wt percent isopleths of halite solubility in single-phase vapor.

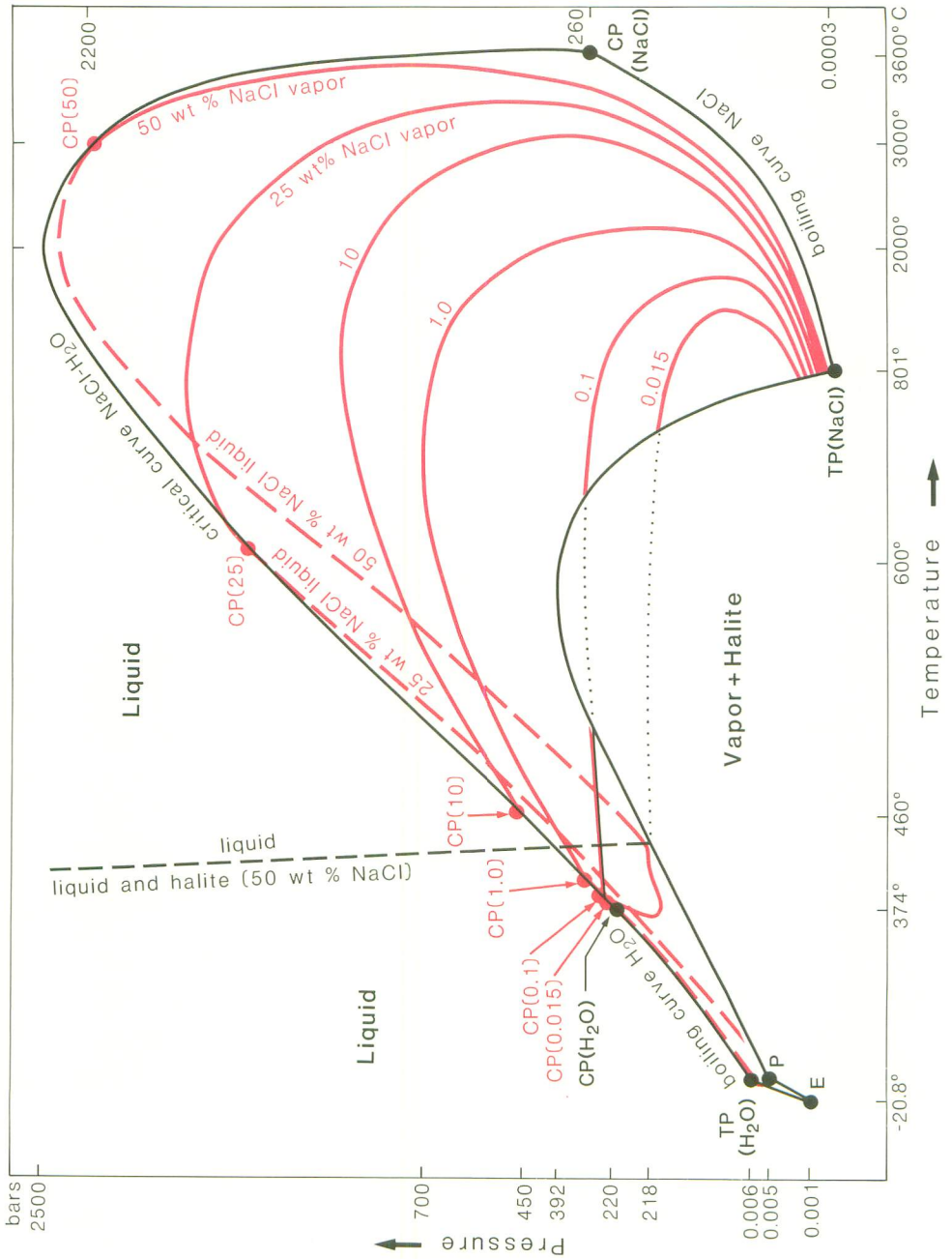
bars
2500
700
450
392
220
218
0.006
0.005
0.001
Pressure
2200
260
0.0003
3600°C
3000°
2000°
801°
600°
460°
374°
-20.8°
Temperature
CP(50)
50 wt % NaCl vapor
25 wt% NaCl vapor
10
1.0
0.1
0.015
CP (NaCl)
boiling curve NaCl
TP(NaCl)
critical curve NaCl-H2O
CP(25)
50 wt % NaCl liquid
25 wt % NaCl liquid
Liquid
Vapor + Halite
liquid
liquid and halite (50 wt % NaCl)
CP(10)
CP(1.0)
CP(0.1)
CP(0.015)
CP(H2O)
boiling curve H2O
TP (H2O)
P
E
Liquid

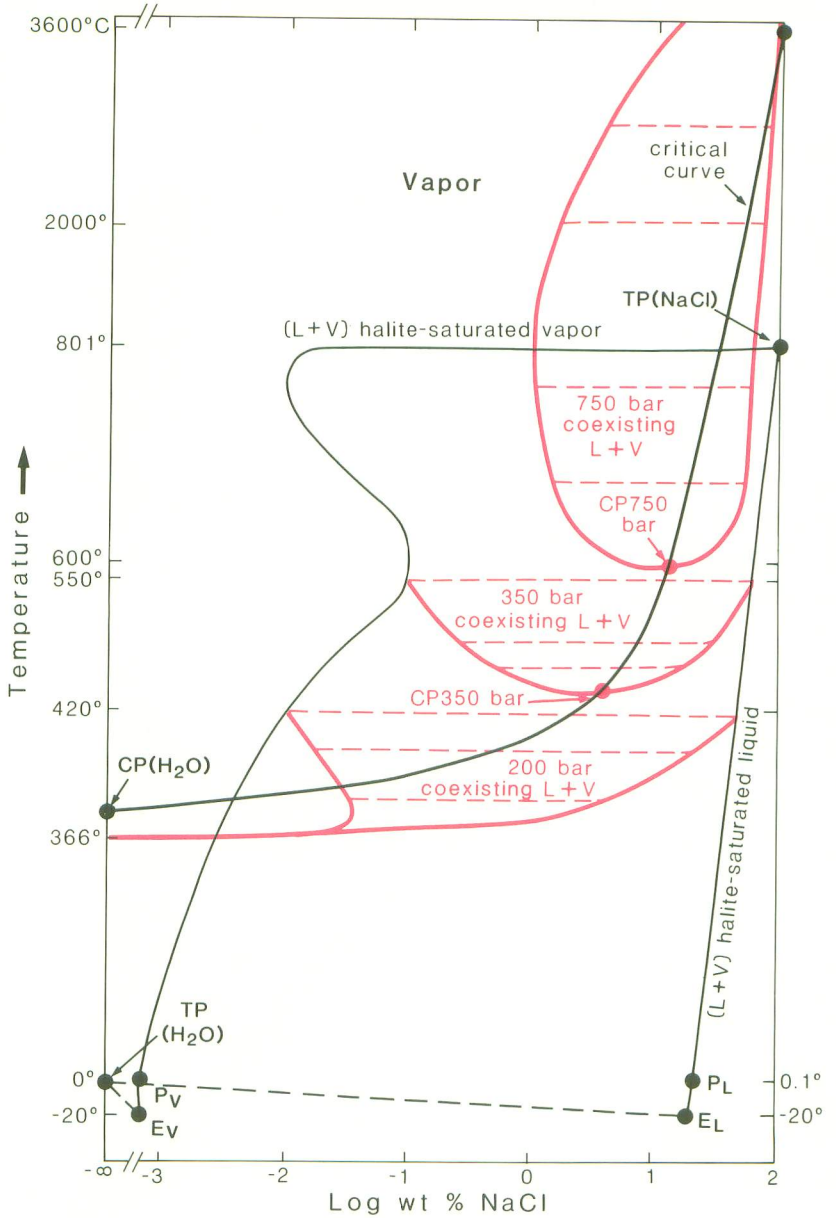

Fig. 1 (B) T-x projection showing three isobars (red lines) on the vapor-liquid coexistence surface. The 350 and 750 isobars are above the critical pressure of H_2O (220 bars) and show critical behavior each with a temperature minimum representing the critical point on the NaCl–H_2O critical line. The 200 bar isobar is below the critical pressure of H_2O and shows no critical behavior with the temperature minimum projecting to the boiling temperature of pure H_2O. Horizontal tie-lines (dashed red lines) on the isobars connect the compositions of coexisting vapors and liquids.

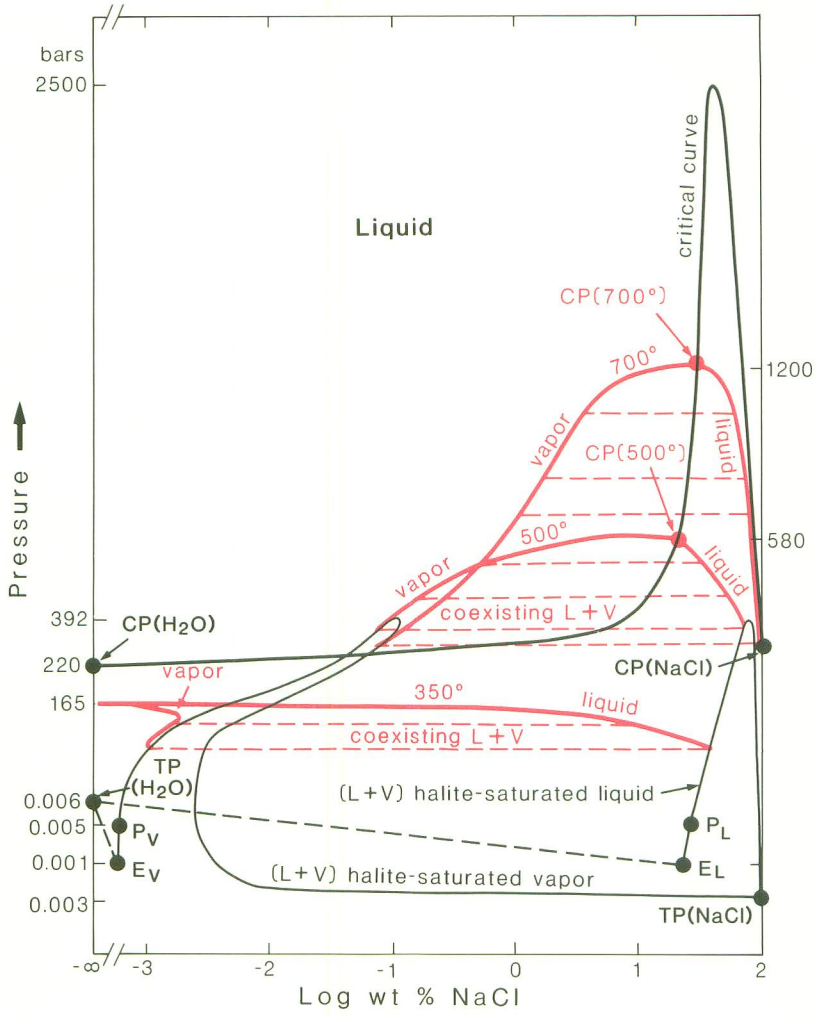

Fig. 1 (C) P-x projection showing three isotherms (red lines) on coexistence surface. The 500° and 700°C isotherms are above the critical temperature of H_2O (374°C) and show critical behavior, each with a pressure maximum representing the critical point on the NaCl–H_2O critical line. The 350°C isotherm is below the critical temperature of H_2O, shows no critical behavior, and has a pressure maximum projecting to the boiling pressure of pure H_2O. Horizontal tie-lines (dashed red lines) on the isotherms connect points representing the compositions of coexisting vapors and liquids.

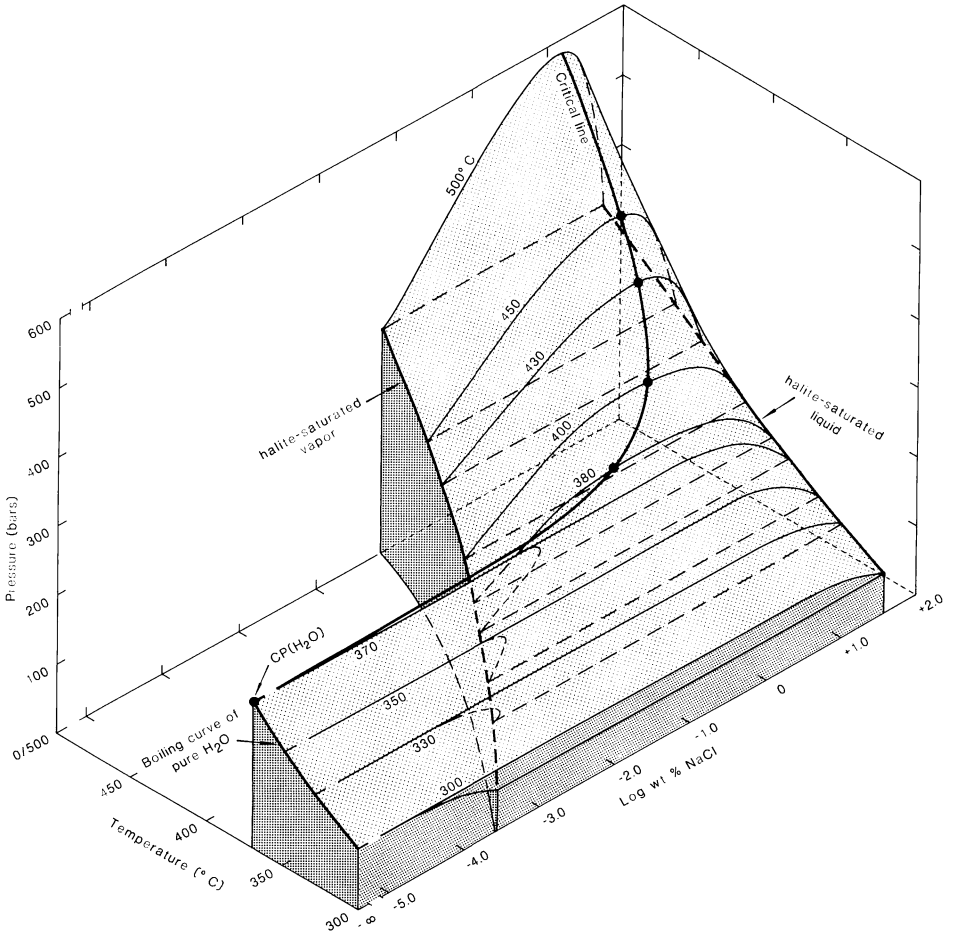

Fig. 2. Perspective view of the P-T-x vapor-liquid surface for the system NaCl–H_2O from 300° to 500°C.

pressure maxima in the critical curve and the three-phase assemblage curve seen in figure 1A are clearly shown. The curve of the three-phase assemblage is again represented by separate liquid and vapor limbs extending from the invariant points (P_L, P_V and E_L, E_V) to the triple point of NaCl. For reference, three isotherms describing coexisting vapors and liquids within the two-phase region are shown, two of which are within the range of the present study. Below the critical temperature of H_2O, represented by the 350°C isotherm, the vapor and liquid limbs extend from the three-phase assemblage points with increasing pressure and meet in a beak-like projection at the boiling pressure of pure water.

Above the critical temperature of water the pattern is changed, as illustrated by the 500° and 700°C isotherms. Vapor and liquid limbs extend from points on the curve of the three-phase assemblage and with increasing pressure meet at the critical point. Horizontal tie-lines describe NaCl contents of coexisting vapors and liquids for particular pressures for each isotherm.

For the range of conditions of the present study (fig. 2) both the critical curve and the curves for the vapor and liquid limbs of the three-phase assembage display no maxima and increase regularly in pressure and wt percent NaCl with temperature increase from 300° to 500°C. The abrupt change in character of the surface from below the critical point of water to above is perhaps more clearly seen in this perspective.

COMPILATION OF EXPERIMENTAL DATA

Method of approach.—Experiments are most conveniently carried out at constant temperature. Therefore, the literature data were compiled on a series of isothermal plots of P versus log wt percent NaCl from 300° to 500°C. Because the two-phase boundary for each isotherm extends from the points on the three-phase assemblage curve either to the boiling point of water or to a point on the NaCl–H_2O critical curve, data for the three-phase assemblage and for the critical curve were compiled separately as a first step. Smoothed curves were then constructed through these compilations, and points were graphically determined for application to each of the isotherms. The vapor and liquid points for each isotherm, and either the boiling point of pure water, or the critical point from the NaCl–H_2O critical line were then plotted on each isotherm to serve as reference points to draw smooth curves through the vapor and liquid limbs. Data from these curves were then smoothed via replotting as isobars and finally as isopleths.

Three-phase assemblage.—Compilation of the T-x relations for three-phase vapor and liquid limbs are shown in figure 3, with the source of the experimental data indicated on the figure. On the vapor side, disagreement between Ölander and Liander (1950) and Sourirajan and Kennedy (1962) prompted the reanalyses by Bischoff, Rosenbauer, and Pitzer (1986), the results of which coincided with those of Ölander and Liander above 450°C and differ sharply in trend from that of Sourirajan and Kennedy. The curve is drawn through the points of this latest study and is projected from 350° down to 300°C, where experimental data are lacking, using the model of Pitzer and Pabalan (1986). On the liquid limb, there is considerable agreement on the position of the curve from 300° to just above 400°C. Above this temperature the data of Urusova (1974, 1975), Chou (1987), and Hall, Sterner, and Bodnar (1987) define a similar trend distinct from the data of Keevil (1942), and a best fit is drawn through this trend. Compilation of the P-T relations for the three-phase assemblage has been presented by Bischoff, Rosen-

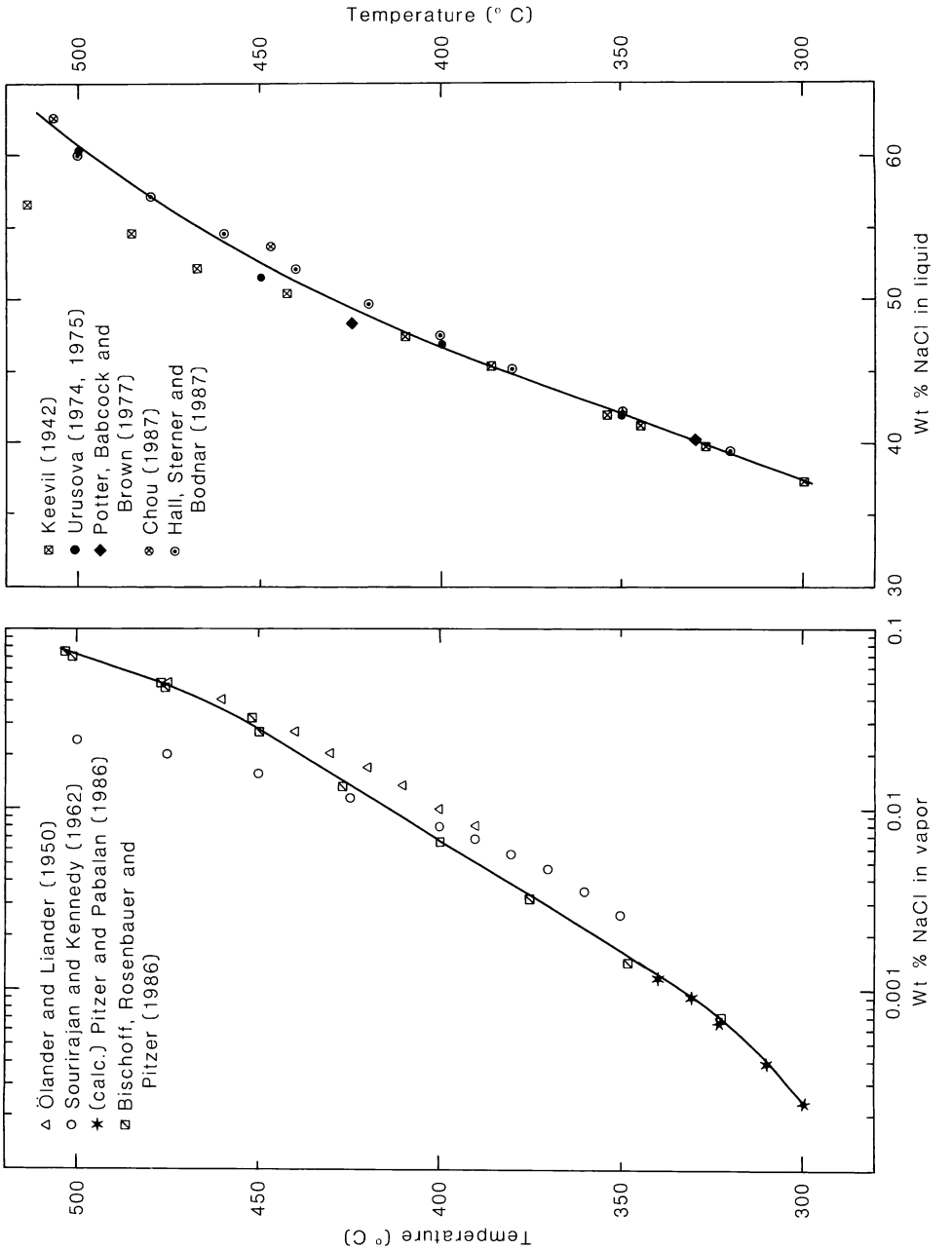
Temperature (° C)
500
450
400
350
300
Keevil (1942)
Urusova (1974, 1975)
Potter, Babcock and Brown (1977)
Chou (1987)
Hall, Sterner and Bodnar (1987)
30
40
50
60
Wt % NaCl in liquid
Ölander and Liander (1950)
Sourirajan and Kennedy (1962)
(calc.) Pitzer and Pabalan (1986)
Bischoff, Rosenbauer and Pitzer (1986)
Temperature (° C)
0.001
0.01
0.1
Wt % NaCl in vapor

bauer, and Pitzer (1986) and shows little scatter among the various investigators.

NaCl–H_2O critical curve.—There is rather good agreement among the various investigators reporting on the P-T projection of the NaCl–H_2O critical line (fig. 4) which is, fortuitously, almost colinear with the saturation-pressure of pure H_2O, and the position of the curve is well constrained. In contrast, data for the T-x projection show considerable scatter (fig. 5) and illustrate the great difficulty there is in experimentally determining the critical composition. Except for Schröer (1927) and Marshall and Jones (1974) who used optical techniques, critical points were estimated from the shape of individually determined isotherms. Critical compositions were estimated by graphically projecting experimentally determined points from both the vapor and liquid limbs. The top of the isotherms are particularly broad in terms of wt percent NaCl, and usually only a few points on the limbs were determined experimentally, these usually at compositions far from the critical composition. Projections, therefore, while relatively accurate for determining critical pressure, are inaccurate for determining critical composition. Because of the considerable scatter, particularly for the temperature interval 450° to 500°C, three isotherms were recently determined with the location of critical composition for each isotherm a major objective (Rosenbauer and Bischoff, 1987). Four additional isotherms with the same objective were recently measured for the temperature range from 380° to 415°C (Bischoff and Rosenbauer, 1988). We consider the critical composition from these two works to be the best constrained and, accordingly, draw the critical line through those points and connect to the critical temperature of pure water.

Subcritical isotherms.—Isotherms are shown for subcritical conditions in figures 6 and 7 and for conditions with critical behavior in figures 8 through 11. The shape of the subcritical isotherms and those with critical behavior are seen to correspond to the shapes indicated in figure 1C. In these isothermal plots coexisting vapors and liquids are represented by imaginary horizontal tie-lines. In each isotherm P-x values for each three-phase vapor and liquid as taken from figure 3 were plotted, as were critical points from figures 4 and 5. For figures 6 and 7 the boiling pressures of pure H_2O were taken from Haar, Gallagher, and Kell (1984). Because the abscissa is in terms of log wt percent NaCl the boiling point of pure H_2O (0 wt percent NaCl) plots at negative infinity. Therefore, the pure H_2O endpoint is represented by an asymptote to which both the liquid and vapor limbs must converge.

For the liquid limbs from 300° to 340°C (fig. 6) there is rather good agreement among the various investigators and the positioning of the liquid phase-boundary is straightforward. On the vapor side, how-

Fig. 3. Compilation of experimental data for three-phase (liquid-vapor-halite) relations for NaCl–H_2O from 300° to 500°C showing curves for both vapor and liquid compositions.

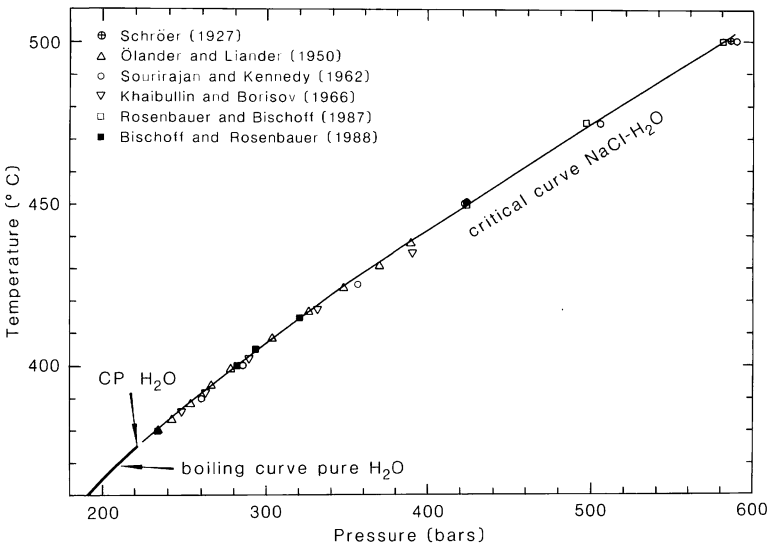

Fig. 4. Compilation of experimental data for NaCl–H_2O critical curve from 300° to 500°C in P-T projection.

ever, there is only the work of Khaibullin and Borisov (1966). The model of Pitzer and Pabalan (1986) provided not only control on the composition of the three-phase vapor but also an estimate of the initial slope of the vapor boundary at pressures immediately above the three-phase vapor point. The boundaries for the vapor limbs, therefore, were drawn from the three-phase points at the calculated initial slopes and then extended as smoothly as possible through the points of Khaibullin and Borisov to the asymptote at the boiling pressure of water. The shapes of the resulting curves are very similar to those predicted theoretically by the model of Tanger and Pitzer (in press). For isotherms at 350° to 370°C (fig. 7) points on the liquid limbs are distributed into two groups. Those of Sourirajan and Kennedy (1962) group with Ölander and Liander (1950), while those of all the others define a slightly different trend. At 350°C, at least, the weight of evidence is overwhelming for the second pattern which was adopted at 360° and 370°C also. It was informative to replot these data as mole-fraction NaCl rather than log wt percent NaCl. On the mole-fraction basis the trend of Sourirajan and Kennedy and of Ölander and Liander show sinusoidal oscillations which seem unreasonable. In contrast, the other data fall on a nearly straight line over the full range from pure H_2O to halite saturation, and the equation of Tanger and Pitzer (in press) shows just that pattern. On the vapor limbs of these isotherms, there is rather good agreement between the data of Khaibullin and Borisov, Ölander and Liander, and the constraints imposed by the three-phase vapor and

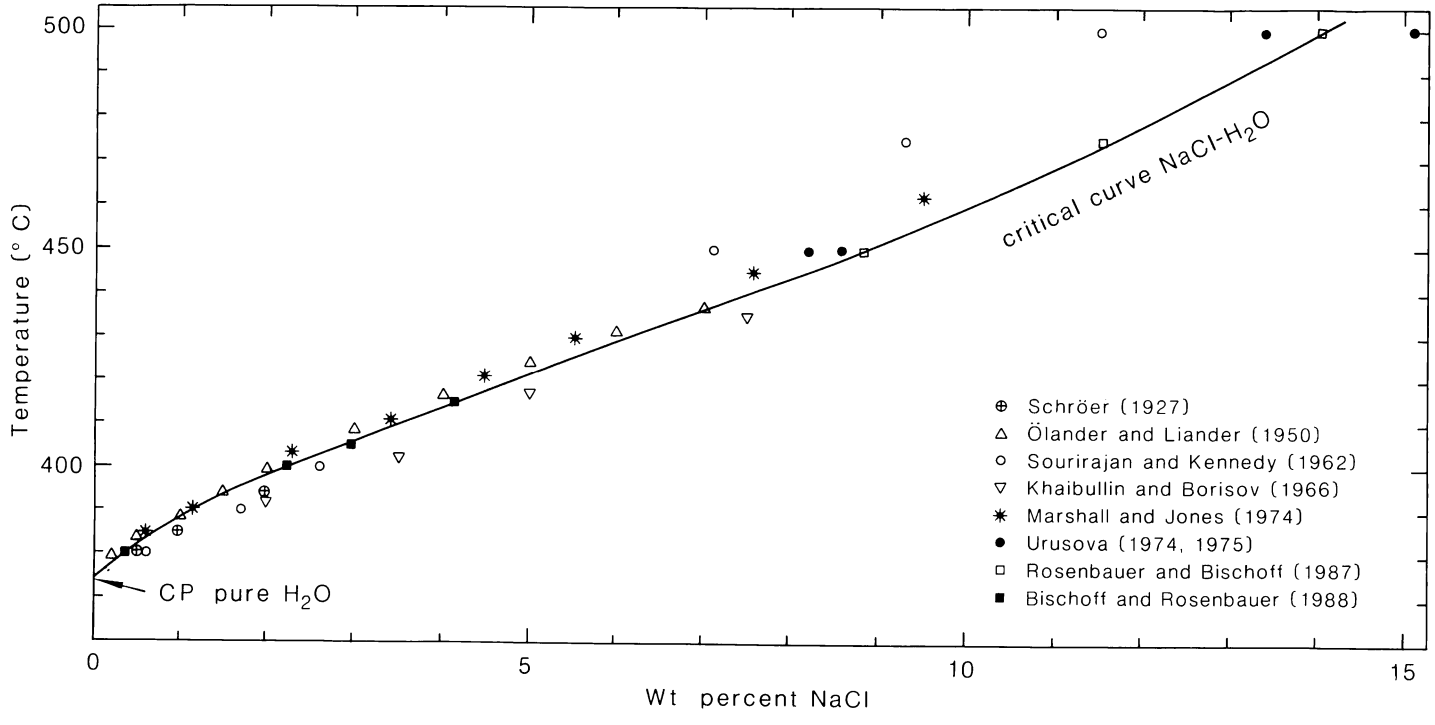

Fig. 5. Compilation of experimental data for NaCl–H_2O critical curve in terms of temperature versus wt percent NaCl.

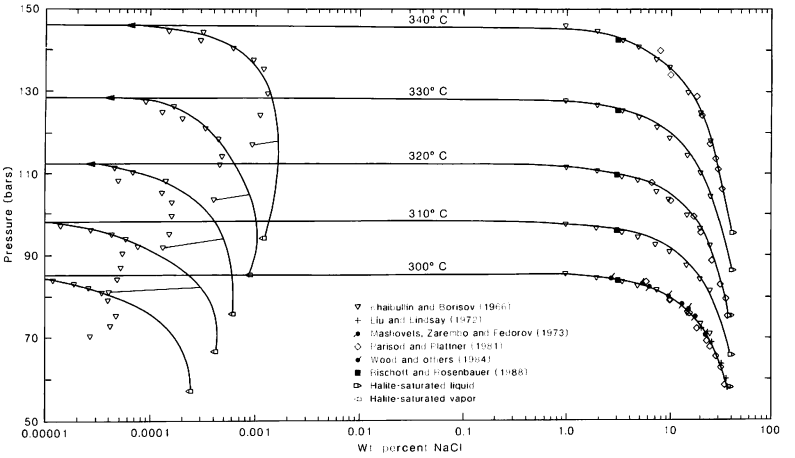

Fig. 6. Compilation of experimental data for vapor-liquid isotherms for NaCl–H_2O for 300° to 340°C. Points for halite-saturated liquids and vapors are taken from curves of figure 3. Phase-boundaries were drawn to project to the boiling pressures of pure H_2O for each temperature taken from Haar and others (1984).

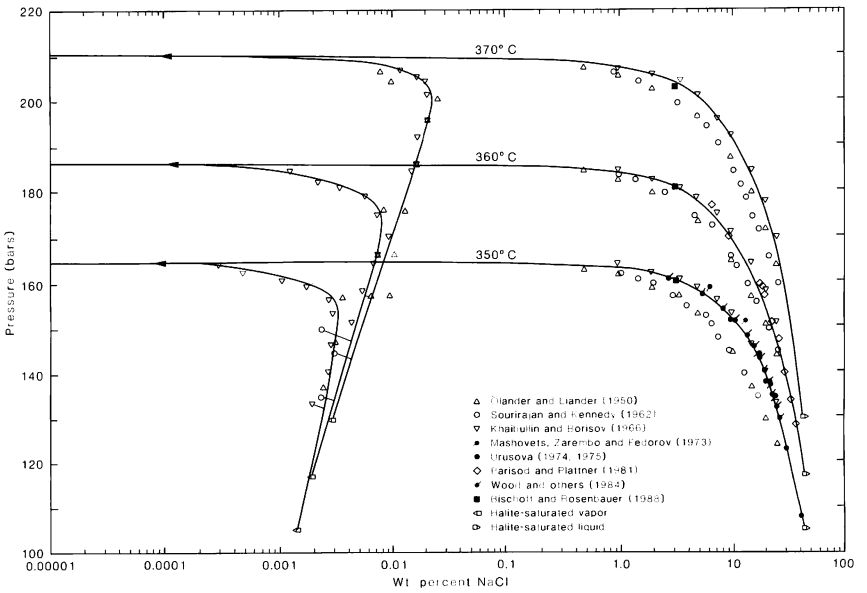

Fig. 7. Compilation of experimental data for vapor-liquid isotherms for NaCl-H_2O for 350° to 370°C. Phase boundaries were drawn to project to the boiling pressures of pure H_2O for each temperature taken from Haar, Gallagher, and Kell (1984).

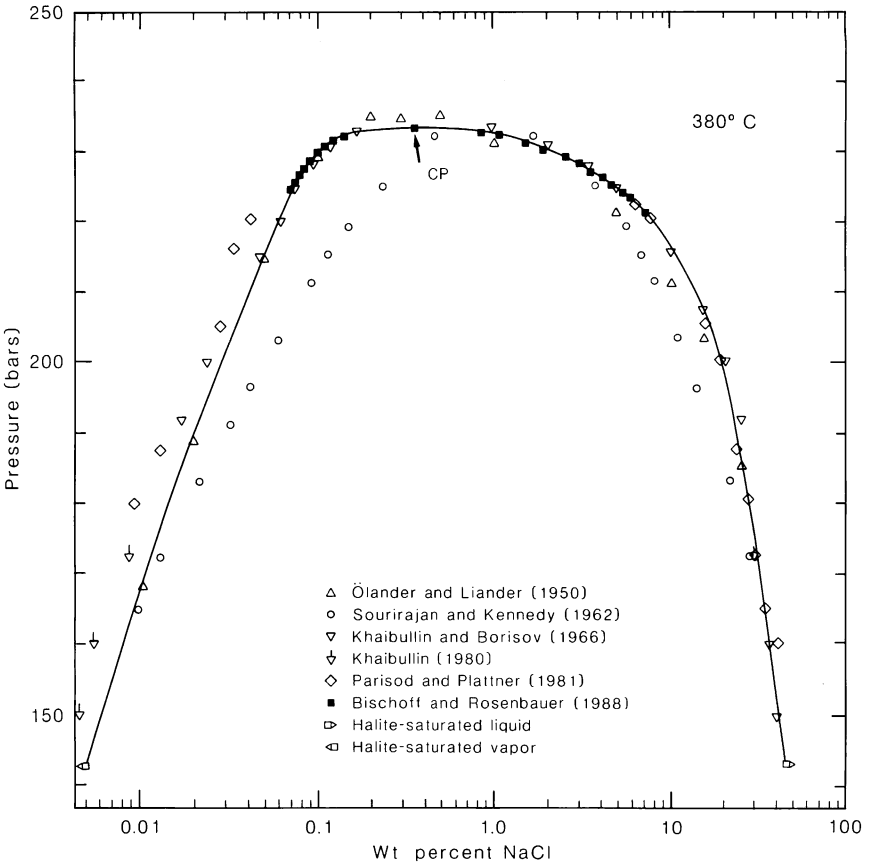

Fig. 8. Compilation of experimental data for 380°C vapor-liquid isotherm of NaCl–H_2O. Critical point is taken from curves in figures 4 and 5, and points for halite-saturated liquid and vapor from curves in figure 3.

the boiling pressures of pure water. Only the data of Sourirajan and Kennedy are at a variance from the curve drawn through these data.

Isotherms with critical behavior.—The transition from subcritical to critical behavior is marked by the loss of the asymptotic beak and the development of dome-shaped isotherms with the critical point at the apex of the dome. Experiments at 373.0° and 375.5°C (Bischoff, Rosenbauer, and Pitzer, 1986) documented the transition in some detail and showed that a memory of the beak in the form of a rounded nose was strongly evident in the 375.5°C isotherm. Figure 8 shows the compilation for the 380° isotherm. Recent experimental work (Bischoff and Rosenbauer, 1988) provides control in the critical region and shows that a slight memory of the subcritical beak still exists at this tempera-

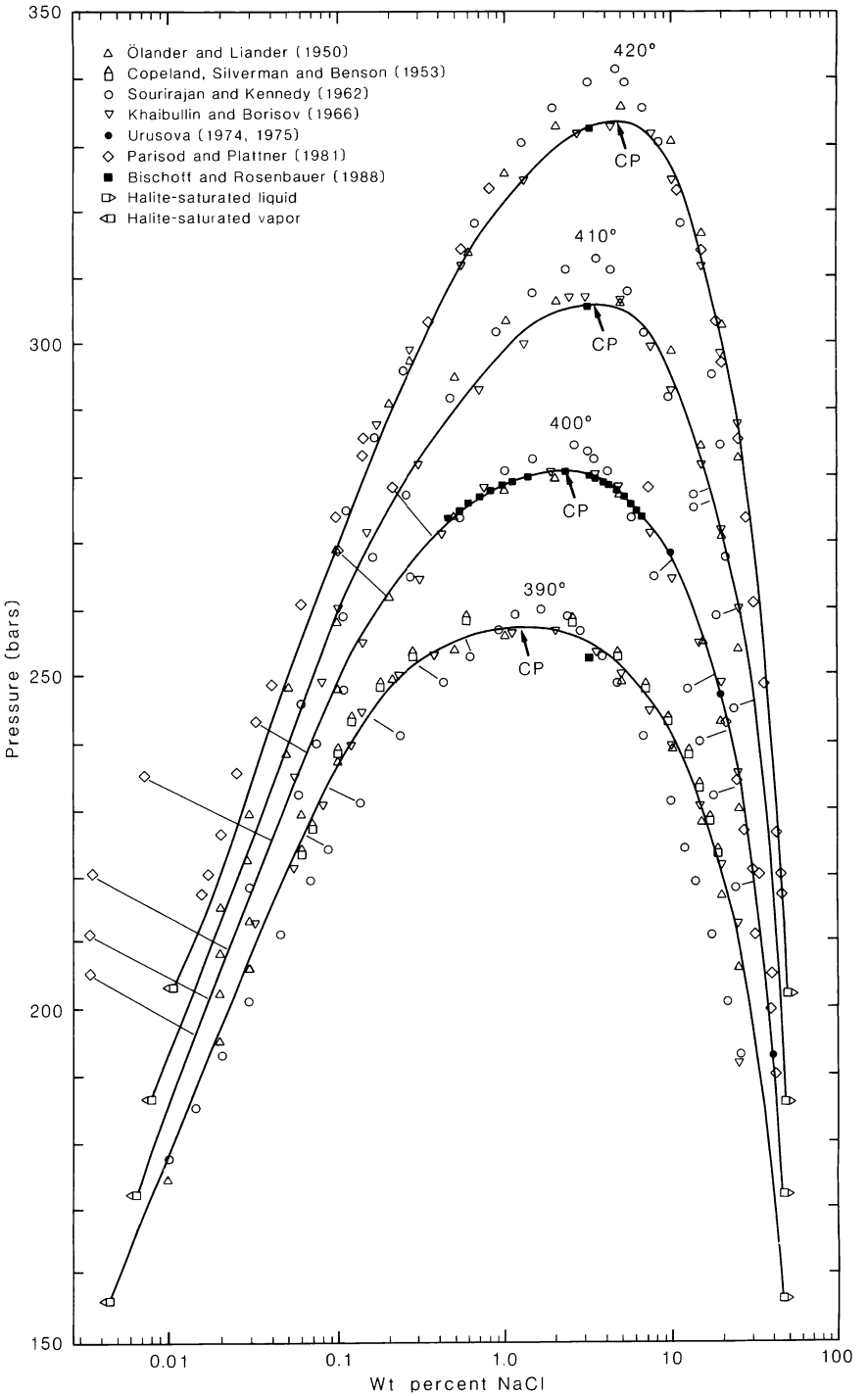

Fig. 9. Compilation of experimental data for vapor-liquid isotherms of NaCl–H_2O from 390° to 420°C. Critical points are taken from curves in figures 4 and 5, and points for halite-saturated liquid and vapor from curves in figure 3.

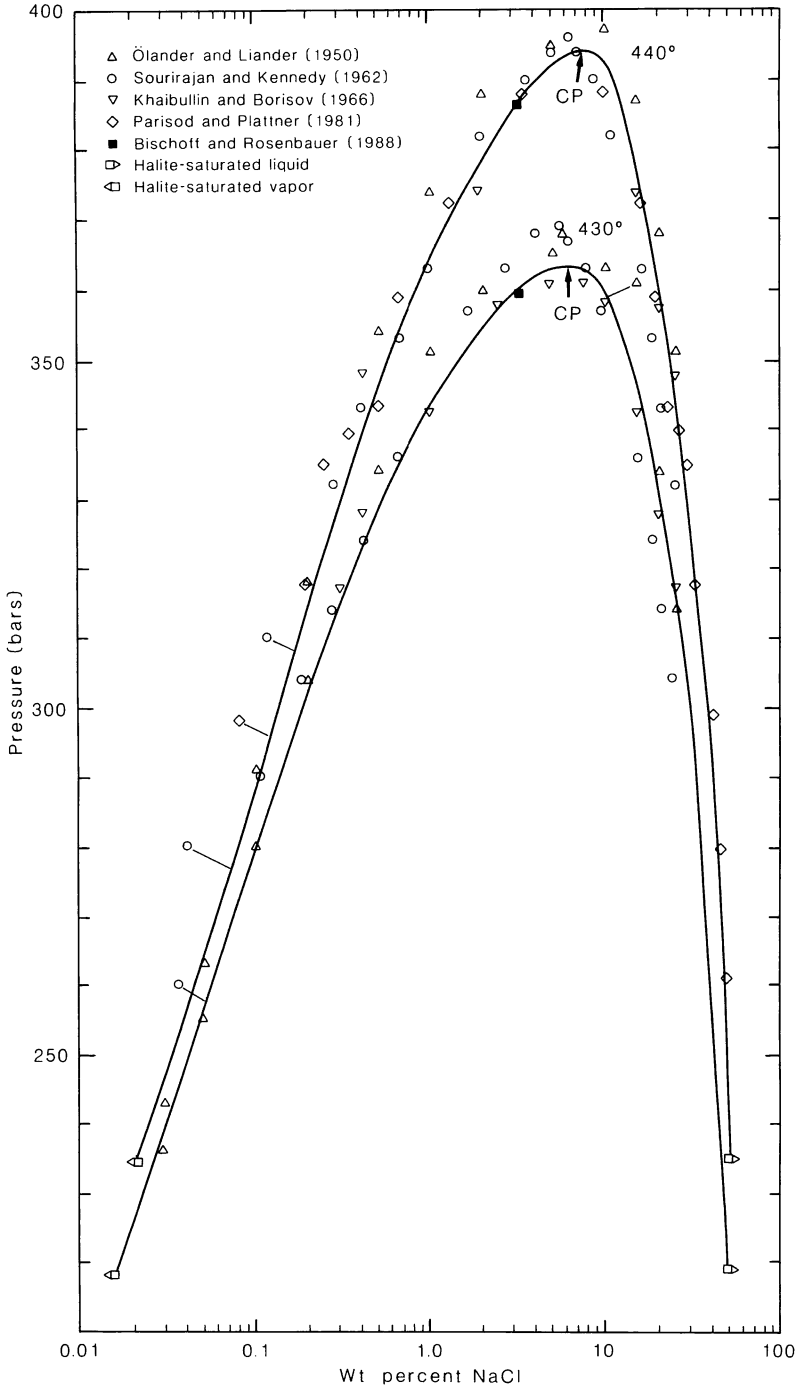

Fig. 10. Compilation of experimental data for vapor-liquid isotherms of NaCl–H_2O for 430° and 440°C. Critical points are from curves in figures 4 and 5, and points for halite-saturated liquids and vapors from curves in figure 3.

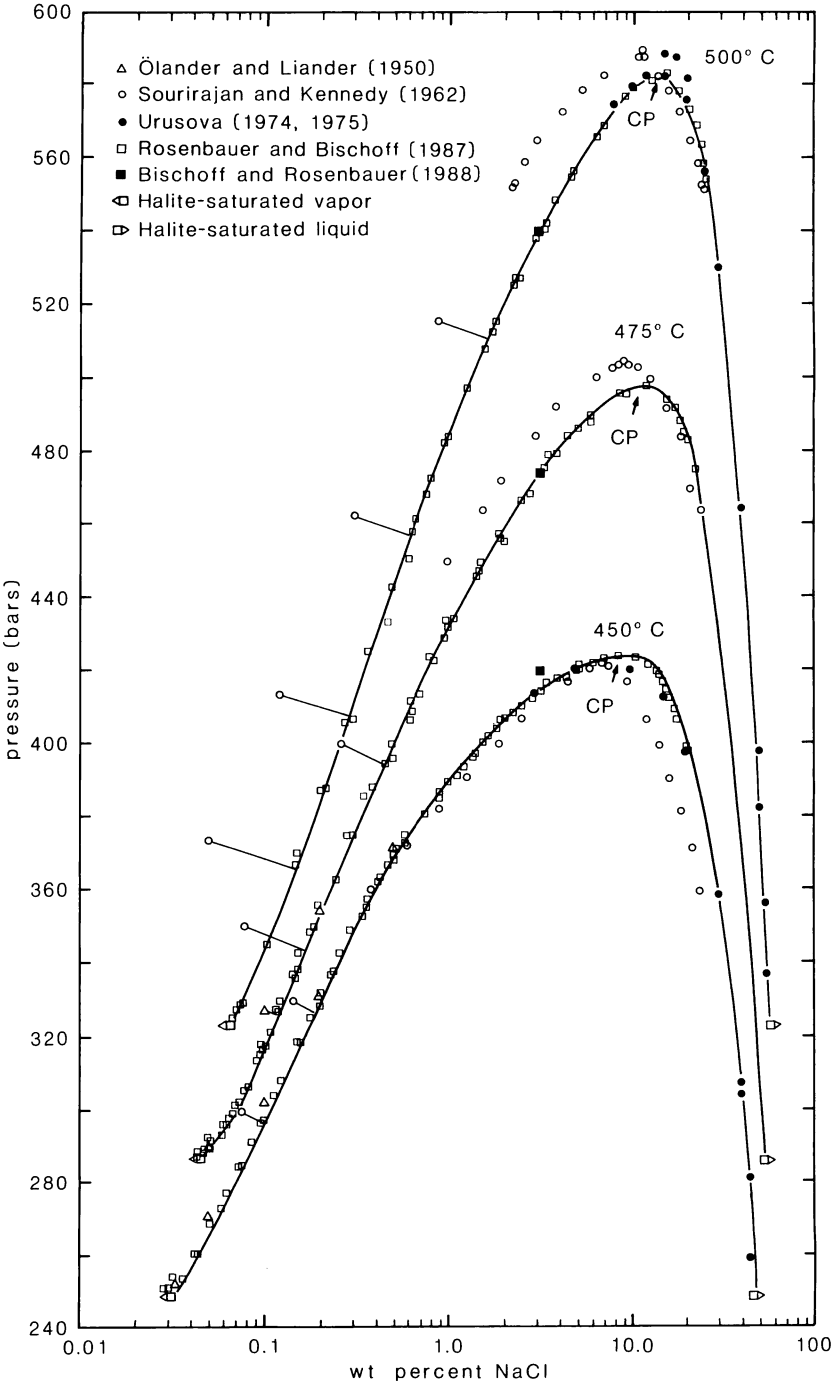

Fig. 11. Compilation of experimental data for vapor-liquid isotherms of NaCl-H_2O from 450° to 500°C. Critical points are from curves in figures 4 and 5, and points for halite-saturated liquids and vapors from curves in figure 3.

ture. On the vapor side a smoothed curve is drawn from the critical region down to the three-phase vapor point through the data points of Ölander and Liander (1950) and Khaibullin and Borisov (1966) and on the liquid side of the three-phase liquid point through data points of Ölander and Liander (1950) and Parisod and Plattner (1981). Isotherms from 390° to 500°C (figs. 9, 10, and 11) show increasing symmetry about the critical regions and enormous expansion of the pressure range from halite saturation to the critical points with increase in temperature. There is reasonable consensus on the liquid limbs of these isotherms with the exception of the data of Sourirajan and Kennedy (1962) who follow the consensus only at 420°, 475°, and 500°C. On the vapor side their data follow the consensus at 400°, 410°, 420°, and 430°C but are sharply discordant at 380°, 390°, 440°, 450°, 475°, and 500°C. Because only Sourirajan and Kennedy reported data on the vapor side at temperatures above 440°C, experiments were carried out by Rosenbauer and Bischoff (1987) to provide additional control on the vapor side and the critical region for these temperatures. Urusova (1974 and 1975) reported data on the critical region and on the liquid limbs at 450° and 500°C, and her work is in good agreement with that of Rosenbauer and Bischoff (1987) where they overlap.

Smoothing of the P-T-x surface.—The composition of coexisting vapor and liquid was graphically determined from each isotherm at 5 bar intervals from the three-phase pressure to either the boiling pressure of pure H_2O or the critical pressure. Smaller pressure intervals were used in the critical region to insure sufficient control for the marked curvature in this region. From the resulting table of P-x values isobaric sections of the two-phase surface were plotted in 10 bar intervals from 100 to 580 bars. Because construction of a single isobar required data for several isotherms, the process revealed some inconsistencies in the earlier choice of phase boundaries on the isotherms. After making initial adjustments on the isotherms, further smoothing was accomplished by making separate isoplethal plots of the liquid and vapor limbs respectively. The curves shown on the isotherms in figures 6 to 11 are the final product of the iteration process, and the results are shown in table 1. Data from this table are shown in isothermal plots in figure 12, isobaric plots in figure 13, and isoplethal plots for the vapor limbs in figure 14.

DISCUSSION

The objective of this study was to produce the table of P-T-x values describing the coexistence liquid-vapor surface of the NaCl–H_2O system, and table 1 is considered the best estimate of these relations that the extant experimental data allow. We consider that the three-phase liquid and vapor curves are reasonably well constrained as are the vapor and liquid limbs of the surface near the three-phase curves. The P-T projection of the critical curve seems to be rather well-constrained. Less confidence, however, is placed on the T-x projection of the critical curve because of the intrinsic difficulty of determining the critical composition

by extrapolation of composition data which are themselves not too precise. Because the phase-boundary in the critical region for each isotherm was controlled by the position of the T-x critical line as constructed in figure 5, it is in this region that the greatest uncertainty and need for further experimental studies exist.

TABLE 1

Pressure-temperature-composition relations for the vapor-liquid region of the system NaCl-H_2O

P,bar	wt % NaCl vapor	wt % NaCl liquid	
	300 °C		
58.0	0.000240	37.50	halite-saturated
60.0	0.000240	35.23	
65.0	0.000220	29.88	
70.0	0.000170	24.19	
75.0	0.000110	17.49	
80.0	0.000050	9.83	
83.0	0.000020	5.04	
84.0	0.000015	3.18	
85.0	0.000007	1.10	
85.8	0.0	0.0	boiling point of pure water
	310 °C		
67.0	0.000400	38.40	halite-saturated
70.0	0.000410	35.14	
75.0	0.000410	30.28	
80.0	0.000350	25.42	
85.0	0.000250	19.49	
90.0	0.000150	13.00	
95.0	0.000070	5.77	
97.0	0.000025	2.55	
98.6	0.0	0.0	boiling point of pure water
	320 °C		
76.0	0.000600	39.30	halite-saturated
80.0	0.000620	35.69	
85.0	0.000600	31.29	
90.0	0.000560	27.01	
95.0	0.000480	22.09	
100.0	0.000370	16.66	
105.0	0.000230	10.81	
110.0	0.000095	3.95	
112.8	0.0	0.0	boiling point of pure water
	330 °C		
86.0	0.00090	40.20	halite-saturated
90.0	0.00096	36.97	
95.0	0.00100	33.11	
100.0	0.00100	29.16	
105.0	0.00087	25.26	
110.0	0.00070	20.60	
115.0	0.00054	15.64	
120.0	0.00038	10.26	
125.0	0.00018	4.25	
128.5	0.0	0.0	boiling point of pure water
	340 °C		
95.0	0.00120	41.20	halite-saturated
100.0	0.00140	37.86	
105.0	0.00155	34.67	
110.0	0.00160	31.29	
120.0	0.00160	24.31	
125.0	0.00150	20.12	
130.0	0.00130	15.89	
135.0	0.00110	11.23	
140.0	0.00068	6.21	
145.0	0.00015	0.50	
145.9	0.0	0.0	boiling point of pure water
	350 °C		
105.0	0.00165	42.20	halite-saturated
110.0	0.00175	39.25	
115.0	0.00190	36.61	
120.0	0.00210	33.73	
125.0	0.00230	30.79	
130.0	0.00245	28.01	
135.0	0.00270	24.75	
140.0	0.00290	21.08	
145.0	0.00310	17.42	
150.0	0.00330	13.54	
155.0	0.00330	9.41	
157.0	0.00310	7.68	
160.0	0.00220	4.71	
163.0	0.00070	2.00	
165.2	0.0	0.0	boiling point of pure water
	360 °C		
117.0	0.0022	43.00	halite-saturated
120.0	0.0023	41.28	
125.0	0.0025	38.80	
130.0	0.0028	36.50	
135.0	0.0030	34.00	
140.0	0.0035	31.30	
145.0	0.0041	28.40	
150.0	0.0048	25.50	
155.0	0.0054	22.50	
160.0	0.0063	19.40	
165.0	0.0072	16.00	
170.0	0.0080	12.40	
175.0	0.0082	8.60	
177.0	0.0078	7.00	
180.0	0.0054	5.00	
183.0	0.0037	2.50	
185.0	0.0015	0.60	
186.5	0.0	0.0	boiling point of pure water

TABLE 1
(Continued)

P,bar	wt % NaCl vapor	wt % NaCl liquid	
	370 °C		
130.0	0.0030	44.00	halite-saturated
135.0	0.0035	41.50	
140.0	0.0041	39.30	
145.0	0.0048	37.10	
150.0	0.0059	34.75	
155.0	0.0065	32.50	
160.0	0.0079	30.00	
165.0	0.0088	27.20	
170.0	0.0105	24.70	
175.0	0.0120	22.00	
180.0	0.0135	18.90	
185.0	0.0155	15.90	
190.0	0.0180	12.50	
195.0	0.0200	9.10	
200.0	0.0230	6.00	
202.0	0.0230	5.00	
205.0	0.0200	3.20	
208.0	0.0100	1.10	
210.3	0.0	0.0	boiling point of pure water
	373 °C		
134.0	0.0033	44.30	halite-saturated
140.0	0.0042	41.25	
145.0	0.0051	39.00	
150.0	0.0062	36.70	
155.0	0.0074	34.50	
160.0	0.0086	32.10	
165.0	0.0100	29.90	
170.0	0.0117	27.40	
175.0	0.0135	25.00	
180.0	0.0155	22.30	
185.0	0.0185	19.50	
190.0	0.0220	16.60	
195.0	0.0250	13.30	
200.0	0.0270	10.00	
205.0	0.0280	6.75	
210.0	0.0280	3.90	
215.0	0.0180	1.20	
216.0	0.0155	0.55	
217.0	0.0110	0.25	
217.5	0.0085	0.18	
217.9	0.0	0.0	boiling point of pure water

P,bar	wt % NaCl vapor	wt % NaCl liquid	
	375.5 °C		
137.0	0.0035	44.50	halite-saturated
140.0	0.0041	43.07	
145.0	0.0051	41.00	
150.0	0.0062	38.90	
155.0	0.0074	36.70	
160.0	0.0086	34.52	
165.0	0.0100	32.20	
170.0	0.0117	29.80	
175.0	0.0135	27.40	
180.0	0.0155	24.80	
185.0	0.0185	22.25	
190.0	0.0220	19.60	
195.0	0.0250	17.00	
200.0	0.0280	14.00	
205.0	0.0340	10.75	
210.0	0.0370	7.50	
215.0	0.0400	4.50	
217.0	0.0410	3.40	
220.0	0.0360	1.75	
222.0	0.0270	0.60	
223.5	0.0900	0.09	critical point
	380 °C		
143.0	0.0040	44.75	halite-saturated
150.0	0.0053	41.69	
155.0	0.0064	39.77	
160.0	0.0076	37.86	
165.0	0.0089	35.78	
170.0	0.0107	33.63	
175.0	0.0127	31.39	
180.0	0.0150	29.05	
185.0	0.0175	26.73	
190.0	0.0208	24.19	
195.0	0.0248	21.66	
200.0	0.0290	19.15	
205.0	0.0350	16.40	
210.0	0.0400	13.54	
215.0	0.0480	10.39	
220.0	0.0580	7.39	
225.0	0.0700	4.56	
230.0	0.1000	1.92	
232.0	0.1250	1.05	
233.2	0.3500	0.35	critical point

(continued p. 238)

Table 1 can be used for charting two-phase behavior in natural systems in a variety of ways. With data presented in 5 bar intervals in table 1 intermediate values of pressure, temperature, and composition may be obtained within the accuracy of the compilation by simple linear interpolation. For illustration, we consider application to seawater (3.2 wt percent NaCl) circulating in seafloor geothermal systems. A P-T section can be constructed through the P-T-x surface at 3.2 wt percent NaCl by appropriate interpolations from table 1 (center curve in fig. 15), and this represents conditions at which seawater first strikes the two-

TABLE 1
(Continued)

P,bar	wt % NaCl vapor	wt % NaCl liquid	
	390 °C		
156.0	0.0050	45.70	halite-saturated
160.0	0.0056	44.49	
165.0	0.0066	42.75	
170.0	0.0080	41.28	
175.0	0.0094	39.50	
180.0	0.0110	37.60	
185.0	0.0132	36.06	
190.0	0.0155	33.80	
195.0	0.0185	31.80	
200.0	0.0220	29.75	
205.0	0.0260	27.50	
210.0	0.0320	25.40	
215.0	0.0380	23.25	
220.0	0.0480	20.85	
225.0	0.0580	18.50	
230.0	0.0720	16.00	
235.0	0.0900	13.35	
240.0	0.1150	10.60	
245.0	0.1650	7.75	
250.0	0.2400	5.10	
255.0	0.5000	2.40	
257.0	1.1800	1.18	critical point
	400 °C		
172.0	0.0065	46.50	halite-saturated
180.0	0.0084	44.18	
185.0	0.0098	42.50	
190.0	0.0115	41.00	
195.0	0.0135	39.50	
200.0	0.0165	38.00	
205.0	0.0190	36.10	
210.0	0.0230	34.25	
215.0	0.0280	32.40	
220.0	0.0330	30.50	
225.0	0.0400	28.60	
230.0	0.0470	26.60	
235.0	0.0580	24.70	
240.0	0.0680	23.50	
245.0	0.0830	20.50	
250.0	0.1000	18.35	
255.0	0.1280	16.15	
260.0	0.1700	13.70	
265.0	0.2400	11.50	
270.0	0.3500	8.60	
275.0	0.5200	6.15	
280.0	1.3500	3.45	
280.7	2.2200	2.22	critical point

P,bar	wt % NaCl vapor	wt % NaCl liquid	
	410 °C		
186.0	0.0080	47.40	halite-saturated
190.0	0.0090	46.32	
195.0	0.0110	45.11	
200.0	0.0130	43.79	
205.0	0.0155	42.43	
210.0	0.0180	41.12	
215.0	0.0215	39.68	
220.0	0.0255	38.30	
225.0	0.0310	36.79	
230.0	0.0360	35.23	
235.0	0.0430	33.63	
240.0	0.0500	31.98	
245.0	0.0600	30.28	
250.0	0.0680	28.64	
255.0	0.0840	26.83	
260.0	0.1000	24.86	
265.0	0.1200	23.06	
270.0	0.1550	21.08	
275.5	0.2000	18.78	
280.0	0.2600	16.91	
285.0	0.3400	14.86	
290.0	0.5000	12.40	
295.0	0.7200	10.00	
300.0	1.0500	8.00	
305.0	2.5000	5.00	
306.0	3.5600	3.56	critical point
	420 °C		
202.0	0.0110	48.80	halite-saturated
205.0	0.0120	48.00	
210.0	0.0145	46.92	
215.0	0.0170	45.80	
220.0	0.0200	44.65	
225.0	0.0240	43.39	
230.0	0.0280	42.10	
235.0	0.0320	40.87	
240.0	0.0370	39.51	
245.0	0.0430	38.12	
250.0	0.0500	36.79	
255.0	0.0600	35.32	
260.0	0.0680	33.82	
265.0	0.0800	32.37	
270.0	0.1000	30.89	
275.0	0.1150	29.26	
280.0	0.1450	27.58	
285.0	0.1700	25.86	
290.0	0.2100	24.08	

phase boundary from the single-phase region. The critical point is seen as an inflection in the P-T curve and is the point at which the 3.2 wt percent NaCl composition plane intersects the NaCl–H_2O critical curve. This point separates the boiling curve from the condensation curve. The upper curve shown in figure 15 describes the composition of the vapor or condensed brine that initially separates from seawater (its conjugate) as a function of temperature.

TABLE 1
(Continued)

P,bar	wt % NaCl vapor	wt % NaCl liquid	
	420 °C		
295.0	0.2500	22.37	
300.0	0.3100	20.60	
305.0	0.3800	18.66	
310.0	0.5000	16.66	
315.0	0.6500	14.70	
320.0	0.8800	12.50	
325.0	1.3000	10.50	
330.0	2.1000	8.20	
334.0	4.7500	4.75	critical point
	430 °C		
218.0	0.0150	50.00	halite-saturated
220.0	0.0170	49.58	
225.0	0.0195	48.52	
230.0	0.0230	47.51	
235.0	0.0270	46.47	
240.0	0.0300	45.42	
245.0	0.0350	44.18	
250.0	0.0410	43.23	
255.0	0.0480	41.94	
260.0	0.0550	40.78	
265.0	0.0640	39.60	
270.0	0.0740	38.39	
275.0	0.0850	36.97	
280.0	0.1000	35.69	
285.0	0.1150	34.39	
290.0	0.1350	33.05	
295.0	0.1600	31.59	
300.0	0.1900	30.08	
305.0	0.2200	28.64	
310.0	0.2600	27.16	
315.0	0.3100	25.64	
320.0	0.3700	24.08	
325.0	0.4400	22.37	
330.0	0.5200	20.60	
335.0	0.6500	18.50	
340.0	0.8100	17.00	
345.0	1.1000	15.00	
350.0	1.5000	13.10	
355.0	2.1000	11.50	
360.0	3.3000	9.50	
363.0	6.1000	6.10	critical point
	440 °C		
235.0	0.023	51.10	halite-saturated
240.0	0.025	50.00	
245.0	0.029	49.23	
250.0	0.034	48.23	
255.0	0.039	47.36	
260.0	0.046	46.40	
265.0	0.053	45.26	
270.0	0.060	44.18	
275.0	0.071	43.23	
280.0	0.080	42.19	

P,bar	wt % NaCl vapor	wt % NaCl liquid	
	440 °C		
285.0	0.092	41.12	
290.0	0.105	39.94	
295.0	0.120	38.91	
300.0	0.135	37.68	
305.0	0.155	36.52	
310.0	0.180	35.32	
315.0	0.200	34.20	
320.0	0.230	32.86	
325.0	0.260	31.49	
330.0	0.300	30.28	
335.0	0.350	28.84	
340.0	0.420	27.37	
345.0	0.480	26.08	
350.0	0.560	24.53	
355.0	0.670	23.17	
360.0	0.830	21.55	
365.0	1.050	19.88	
370.0	1.300	18.20	
375.0	1.650	16.50	
380.0	2.200	15.00	
385.0	2.900	13.50	
390.0	4.200	11.20	
394.0	7.500	7.50	critical point
	450 °C		
250.0	0.030	52.50	halite-saturated
255.0	0.035	51.50	
260.0	0.040	50.80	
265.0	0.045	49.93	
270.0	0.051	49.09	
275.0	0.058	48.23	
280.0	0.068	47.36	
285.0	0.074	46.47	
290.0	0.082	45.57	
295.0	0.093	44.65	
300.0	0.104	43.71	
305.0	0.115	42.75	
310.0	0.130	41.78	
315.0	0.145	40.78	
320.0	0.158	39.77	
325.0	0.175	38.74	
330.0	0.200	37.50	
335.0	0.220	36.42	
340.0	0.250	35.32	
345.0	0.290	34.20	
350.0	0.320	33.05	
355.0	0.360	31.88	
360.0	0.410	30.69	
365.0	0.470	29.47	
370.0	0.540	28.22	
375.0	0.650	26.94	
380.0	0.780	25.42	
385.0	0.930	24.08	
390.0	1.150	22.50	
395.0	1.400	21.31	
400.0	1.700	20.00	
405.0	2.150	18.50	
410.0	2.750	17.10	
415.0	3.600	15.40	
420.0	5.500	12.60	
423.0	8.800	8.80	critical point

(continued p. 240)

TABLE 1
(Continued)

P,bar	wt % NaCl vapor	wt % NaCl liquid	
	475 °C		
286.0	0.045	56.20	halite-saturated
290.0	0.050	55.80	
295.0	0.056	55.00	
300.0	0.065	54.31	
305.0	0.074	53.54	
310.0	0.080	52.90	
315.0	0.090	52.24	
320.0	0.100	51.44	
325.0	0.110	50.76	
330.0	0.120	50.07	
335.0	0.132	49.23	
340.0	0.145	48.52	
345.0	0.160	47.80	
350.0	0.180	46.92	
355.0	0.197	46.17	
360.0	0.220	45.42	
365.0	0.240	44.49	
370.0	0.270	43.71	
375.0	0.290	42.75	
380.0	0.340	41.94	
385.0	0.370	41.12	
390.0	0.400	40.11	
395.0	0.450	39.25	
400.0	0.500	38.21	
405.0	0.550	37.33	
410.0	0.630	36.42	
415.0	0.680	35.51	
420.0	0.770	34.39	
425.0	0.850	33.44	
430.0	0.970	32.28	
435.0	1.050	31.29	
440.0	1.200	30.28	
445.0	1.350	29.26	
450.0	1.550	28.01	
455.0	1.720	26.94	
460.0	1.980	25.70	
465.0	2.200	24.80	
470.0	2.650	23.50	
475.0	3.200	22.00	
480.0	3.900	21.00	
485.0	5.000	19.00	
490.0	6.500	17.00	
495.0	9.100	13.60	
496.8	11.300	11.30	critical point
	500 °C		
324.0	0.068	60.70	halite-saturated
330.0	0.076	60.00	
335.0	0.084	59.40	
340.0	0.094	58.99	

P,bar	wt % NaCl vapor	wt % NaCl liquid	
	500 °C		
345.0	0.105	58.30	
350.0	0.115	57.72	
355.0	0.125	57.25	
360.0	0.135	56.65	
365.0	0.154	56.05	
370.0	0.165	55.31	
375.0	0.175	54.69	
380.0	0.190	54.18	
385.0	0.200	53.54	
390.0	0.225	52.90	
395.0	0.240	52.24	
400.0	0.260	51.64	
405.0	0.275	50.90	
410.0	0.300	50.21	
415.0	0.330	49.51	
420.0	0.350	48.81	
425.0	0.380	48.09	
430.0	0.410	47.51	
435.0	0.440	46.62	
440.0	0.480	46.02	
445.0	0.520	45.26	
450.0	0.560	44.49	
455.0	0.620	43.71	
460.0	0.670	42.91	
465.0	0.720	42.10	
470.0	0.800	41.28	
475.0	0.860	40.45	
480.0	0.950	39.60	
485.0	1.000	38.74	
490.0	1.100	37.86	
495.0	1.250	36.97	
500.0	1.350	36.06	
505.0	1.500	35.14	
510.0	1.650	34.20	
515.0	1.850	33.25	
520.0	2.050	32.47	
525.0	2.250	31.29	
530.0	2.550	30.18	
535.0	2.900	29.16	
540.0	3.300	28.10	
545.0	3.700	27.20	
550.0	4.200	26.30	
555.0	4.700	25.00	
560.0	5.300	23.60	
565.0	6.100	22.50	
570.0	7.000	21.00	
575.0	8.500	19.00	
580.0	11.000	16.35	
581.8	13.600	13.60	critical point

During circulation between the seafloor and the roofs of magma chambers, two possible ways seawater may strike the two-phase boundary are by rapid heating (flashing) or by decompression. Flashing might occur as seawater is abuptly brought into contact with molten magma, as during intrusion. We consider a parcel of seawater circulating at 450

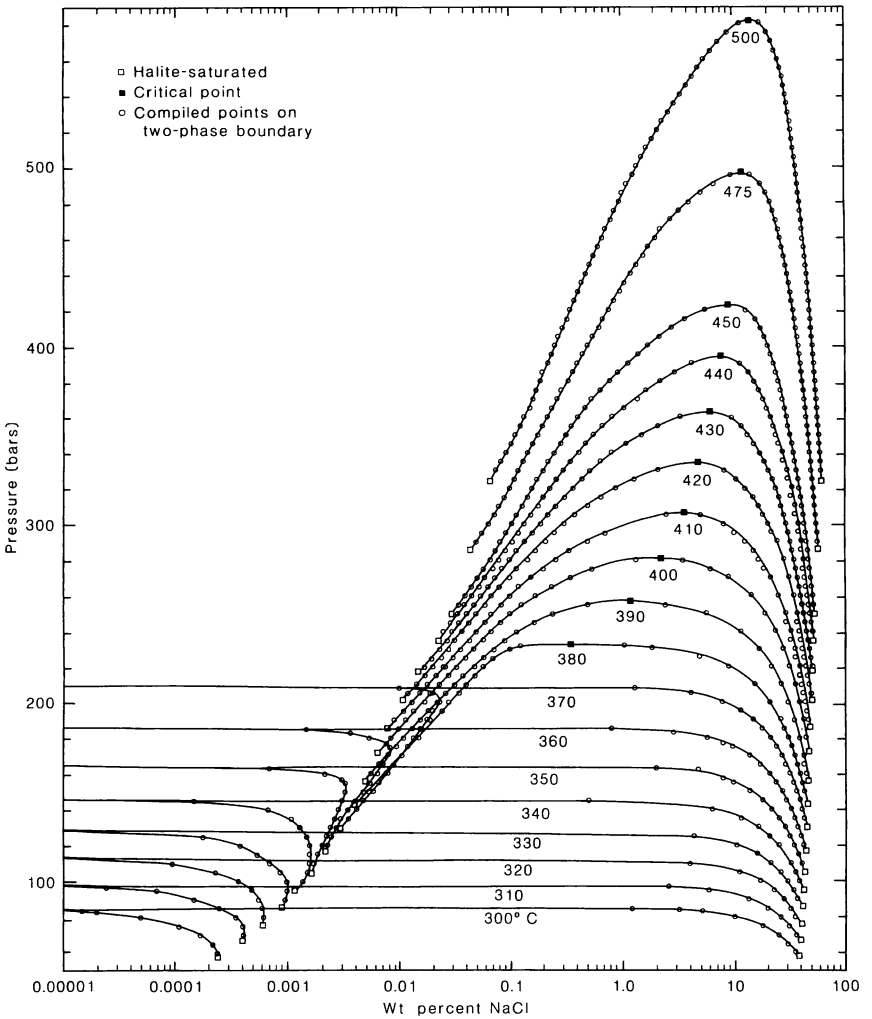

Fig. 12. Isotherms of the vapor-liquid region of NaCl–H_2O from 300° to 500°C as compiled and smoothed from figures 6 to 11. Individual points are from table 1.

bars a typical hydrostatic pressure at the top of a magma chamber of a seafloor spreading center and at a temperature of 400°C as shown by point A in figure 15. If the seawater is subject to flashing, the temperature will simply rise abruptly at constant pressure to point B where the two-phase boundary is struck at 464°C. At this point seawater strikes the P-T curve as a vapor, and the initial conjugate is a liquid (point B′) of 19.5 wt percent NaCl. In the case of decompression, the single phase

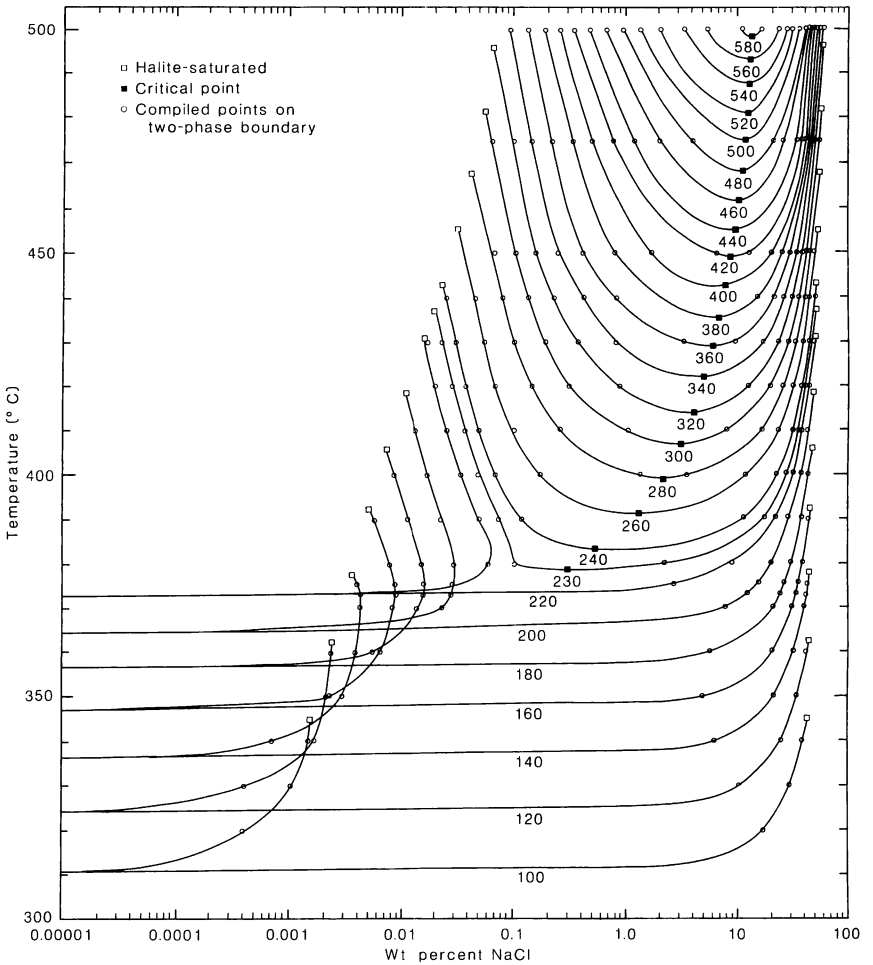

Fig. 13. Isobars of the vapor-liquid region of NaCl–H_2O from 100 to 580 bars as compiled and smoothed from figures 6 to 11. Individual points are from table 1.

seawater begins to rise from point A, and, as a consequence, the pressure decreases. In isentropic adiabatic decompression, temperature drops in a predictable manner with decreasing pressure, and the relation between P and T can be calculated from entropy values presented by Bischoff and Rosenbauer (1985) for single phase seawater. The two-phase boundary is struck at point C, at 375 °C and 218 bars. This point is on the boiling curve, below the seawater critical point, and the initial conjugate is a vapor at point C′ of 0.04 wt percent NaCl. If the mixture rises adiabatically and remains as a closed system, then the system will remain on the two-phase surface thereafter, and the composition of the

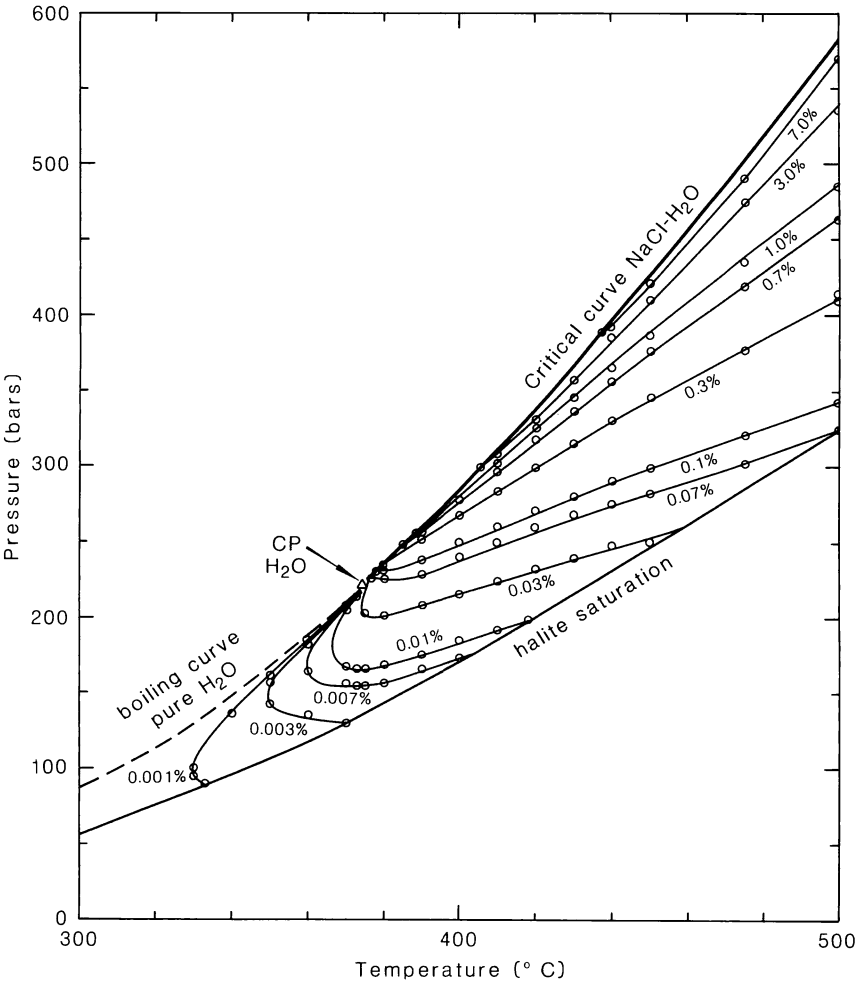

Fig. 14. Isoplethal plots of wt percent NaCl in vapors of vapor-liquid region of NaCl–H_2O as a function of temperature and pressure. Points are taken from table 1 by linear interpolation.

coexisting liquids and vapors will be described by the tie-lines. Because hydrostatic pressure is a simple function of water depth in these systems, the position of the system on the two-phase surface is most readily visualized in terms of isobars (figs. 13 and 16). Horizontal tie-lines describe the wt percent NaCl for the liquid-vapor pair for any given pressure and temperature, and a mass fraction of each is calculated by a simple mass balance equation,

$$X_l = (S_{sw} - S_v)/(S_l - S_v)$$

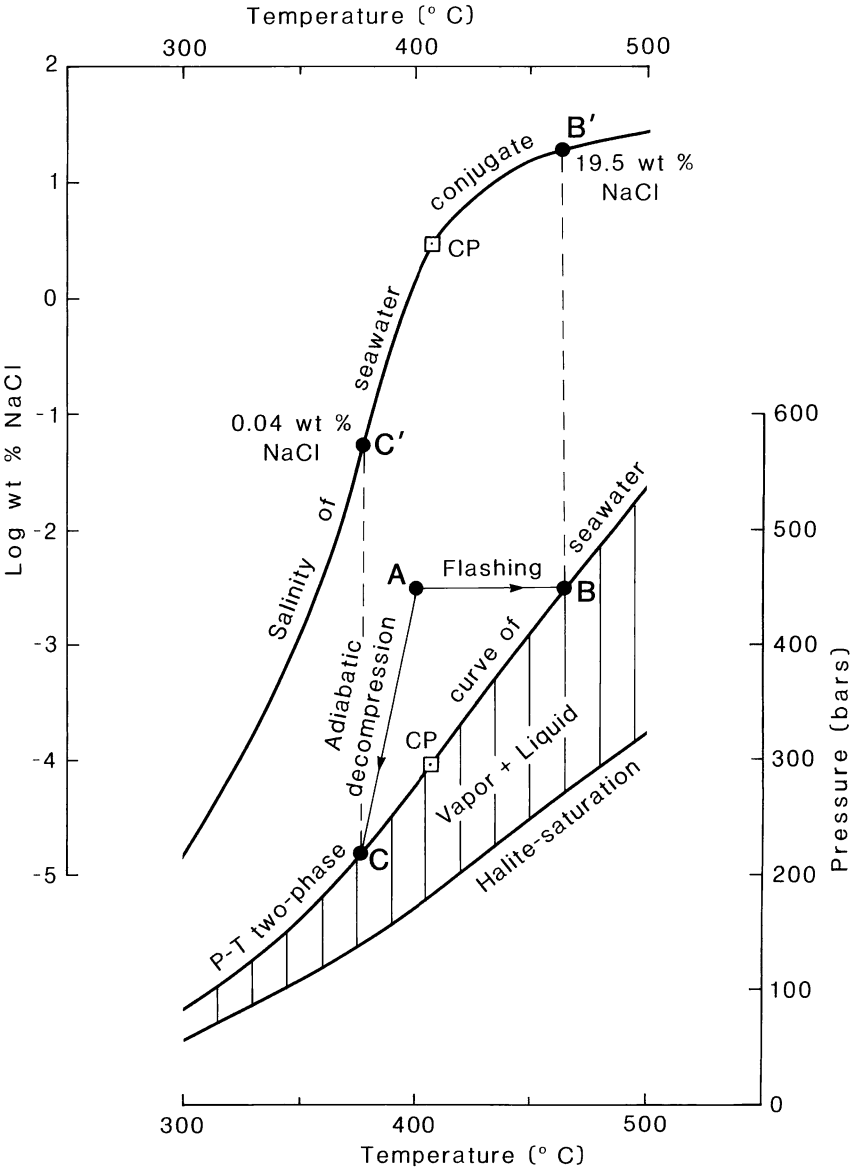

Fig. 15. P-T two-phase boundary of seawater (3.2 wt percent NaCl) and curve showing log wt percent NaCl of the conjugate fluid at the point of initial phase-separation of seawater as a function of temperature, as constructed from data in table 1. Conjugate fluid is a liquid at temperatures above the critical temperature and a vapor below.

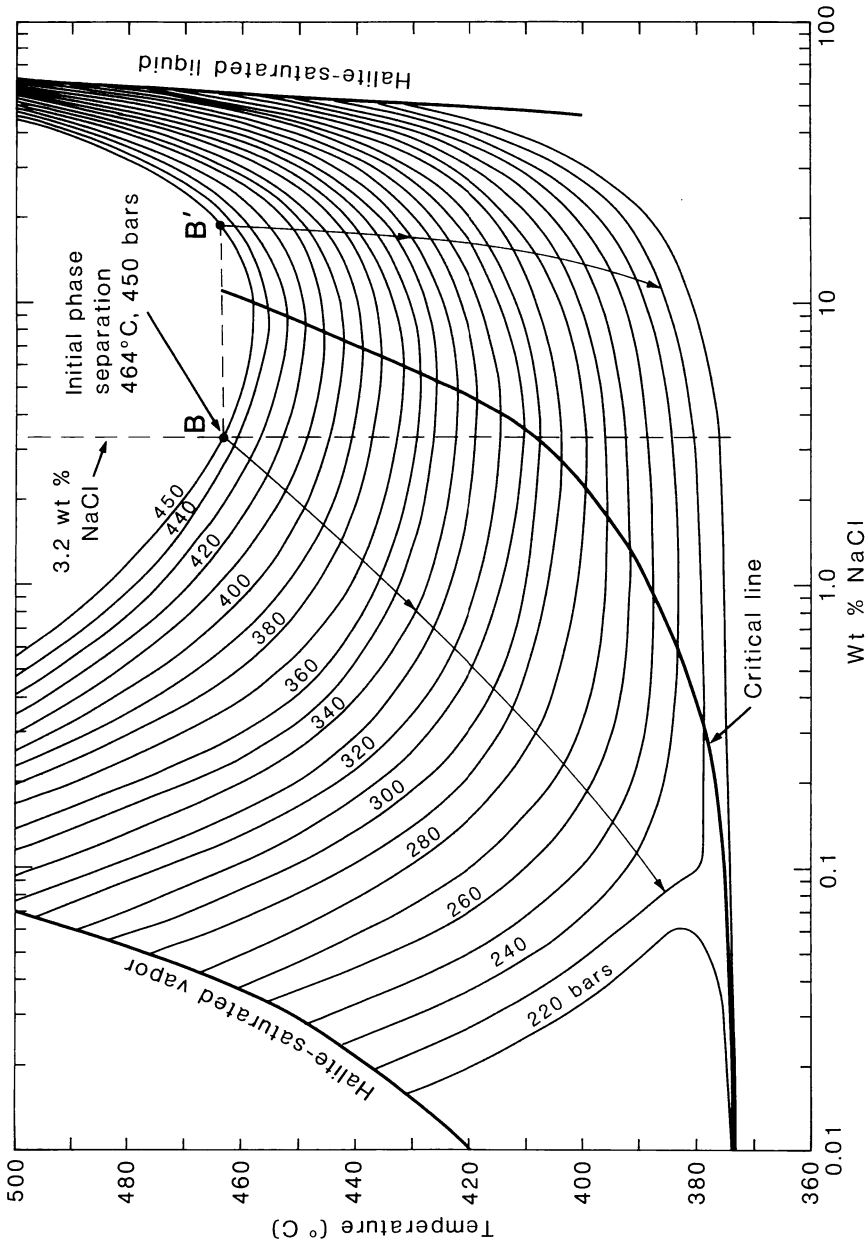

Fig. 16. Isobaric diagram of two-phase region of NaCl–H_2O from 220 to 450 bars showing approximate trajectory of closed system vapor-liquid resulting from flashing of seawater at 464°C and 450 bars (point B) and subsequent adiabatic decompression. Trajectory calculated from equation of Tanger and Pitzer (in press).

where X_l is the mass fraction of the liquid, S is the wt percent NaCl, and the subscripts sw, v, and l refer to seawater (3.2 wt percent NaCl), vapor, and liquid. The weight fraction of the vapor is simply $1 - X_l$.

The exact trajectory of the system depends on the degree of energy loss or gain by the system and whether isolation of the two phases followed by mixing with colder seawater occurs. Information can be gained from table 1 for any given pressure (specified depth) provided that either temperature or the salinity of either the vapor or liquid is known. In the extreme case of closed-system adiabatic decompression in which entropy is conserved, a trajectory on the P-T-x surface can be quantified if entropy of the coexisting vapors and liquid are known, as was done in a preliminary fashion in an earlier work (Bischoff and Pitzer, 1985). The trajectory of an adiabatic decompression of the flashed seawater from point B in figure 15 is shown semiquantitatively in figure 16 down to a pressure of 230 bars, using vapor-liquid entropies calculated by the model of Tanger and Pitzer (in press). An interesting feature of this trajectory is that the salinity of the liquid gradually decreases with decompression from that originally separated at point B. At 230 bars, a typical pressure at seafloor depths along spreading centers at which hydrothermal vents occur, the temperature of the vapor-liquid mixture will be approx 386°C, the mass-fraction of liquid will be about 26 percent, and the liquid will have a salinity of about 12 wt percent NaCl, and the vapor about 0.08 wt percent NaCl. Further and more accurate calculations of this type will have application to specific conditions of particular seafloor systems but will require more accurate thermochemical information on the coexisting vapors and liquids.

ACKNOWLEDGMENTS

Robert Rosenbauer and John Fitzpatrick provided much useful assistance with data manipulation. Figures were drawn by Briget Fulop and Phyllis Swenson. The manuscript benefited from particularly careful and thoughtful critical reviews by I-Ming Chou, William Evans, and Robert Bodnar. The work at Berkeley was supported by the Director, Office of Energy Research, Office of Basic Energy Sciences, Division of Engineering and Geosciences, of the U.S. Department of Energy, under contract number DE-ACO3-76SF00098.

REFERENCES

Bischoff, J. L., and Pitzer, K. S., 1985, Phase relations and adiabats in boiling seafloor geothermal systems: Earth and Planetary Science Letters, v. 75, p. 327–338.

Bischoff, J. L., and Rosenbauer, R. J., 1985, An empirical equation of state for hydrothermal seawater (3.2% NaCl): American Journal of Science, v. 285, p. 725–763.

———— 1988, Liquid-vapor relations in the critical region of the system NaCl–H_2O 380° to 415°C: a refined determination of the critical point and the two-phase boundary of seawater: Geochimica et Cosmochimica Acta, v. 53, p. 2121–2126.

Bischoff, J. L. Rosenbauer, R. J., and Pitzer, K. S., 1986, The system NaCl–H_2O: relations of vapor-liquid near the critical temperature of water and of vapor–liquid–halite from 300° to 500°C: Geochimica et Cosmochimica Acta, v. 50, p. 1437–1444.

Bodnar, R. J., Burnham, C. W., and Sterner, S. M., 1985, Synthetic fluid inclusions in natural quartz. III. determination of phase equilibrium properties in the system H_2O–NaCl to 1000°C and 1500 bars: Geochimica et Cosmochimic Acta, v. 49, p. 1861–1873.

Chase, M. W., Jr., Davies, C. A., Downery J. R. Jr., Frurip, D. J., McDonald, R. A., and Syverud, A. N., 1985, JANAF Tables, 3d ed.: Journal of Physical Chemistry Reference Data, v. 14, Supplement no. 1, 1856p.

Chou, I-M., 1987, Phase relations in the system NaCl–KCl–H_2O III: solubilities of halite in vapor-saturated liquids above 445°C and redetermination of phase equilibrium properties in the system NaCl–H_2O to 1000°C and 1500 bars: Geochimica et Cosmochimica Acta, v. 51, p. 1965–1975.

Copeland, C. S., Silverman, J., and Benson, S. W., 1953, The system NaCl–H_2O at supercritical temperatures and pressures: Journal of Chemical Physics, v. 21, p. 12–16.

Delaney, J. R., Mogk, D. W., and Mottl, M. J., 1987, Quartz-cemented breccias from the Mid-Atlantic Ridge: samples of a high-salinity hydrothermal zone: Journal of Geophysical Research, v. 92, p. 9175–9191.

Fournier, R. O., 1987, Conceptual models of brine evolution in magmatic-hydrothermal systems: United States Geological Survey Professional Paper 1350, chap. 55, p. 1487–1506.

Haar, L., Gallagher, J. S., and Kell, G., 1984, NBS/NRC Steam Tables: Thermodynamic and transport properties and computer programs for vapor and liquid states of water in SI units: Washington, Hemisphere, 320 p.

Hall, D. L., Sterner, S. M., and Bodnar, R. J., 1987, Phase equilibria in the system NaCl–KCl–H_2O [abs.]: Eos, v. 68, p. 450.

Keevil, N. B., 1942, Vapor pressures of aqueous solutions at high temperatures: American Chemical Society Journal, v. 64, p. 841–850.

Khaibullin, Kh., 1980, Tablitsi termodinamicheskikh cvoistv gazov i zhidkostei, vuipusk 6, vodnie i parofaznie rastvorui sistema voda-khloristuii natrii (Tables of thermodynamic characteristics of gases and liquids, issue 6, liquid and vapor solutions of the system NaCl-H_2O): Moscow, Izdatel'stvo Standartov, 80 p.

Khaibullin, Kh., and Borisov, N. M., 1966, Experimental investigation of the thermal properties of aqueous and vapor solutions of sodium and potassium chlorides at phase equilibrium: Teplofizika Vysokikh Temperatur, v. 4, p. 518–523 (English translation, p. 489–494).

Linke, W. F., 1965, Solubilities Inorganic and Metal-Organic Compounds, Volume II, 4th ed.: Washington, D. C., American Chemical Society. p. 958–959.

Liu, C-t., and Lindsay, W. T. Jr., 1972, Thermodynamics of sodium chloride solutions at high temperatures: Journal of Solution Chemistry, v. 1, p. 45–69.

Marshall, W. L., and Gill, J. S., 1974, Effect of pressure on liquid-liquid immiscibility of high temperature aqueous solution mixtures of uranyl sulfate and sulfuric acid, 280–450°C, 75–1800 bars; Journal of Inorganic and Nuclear Chemistry, v. 36, p. 2303–2312.

Marshall, W. L., and Jones, E. V., 1974, Liquid-vapor critical temperatures of aqueous electrolyte solutions: Journal of Inorganic and Nuclear Chemistry, v. 36, p. 2313–2318.

Mashovets, V. P., Zarembo, V. I., and Fedorov, M. K., 1973, Vapor pressures of aqueous solutions of NaCl, NaBr, and NaI at temperatures in the range 150–350°: Journal of Applied Chemistry, USSR, v. 46, p. 684–686. (English translation).

Morey, G. W., 1957, The solubility of solids in gases: Economic Geology, v. 52, p. 225–251.

Ölander, A., and Liander, H., 1950, The phase diagram of sodium chloride and steam above the critical point: Acta Chemica Scandinavica, v. 4, p. 1437–1445.

Parisod, C. J., and Plattner, E., 1981, Vapor-liquid equilibria of the NaCl–H_2O system in the temperature range 300–440°C: Journal of Chemical Engineering Data, v. 26, p. 16–20.

Pitzer, K. S., 1984, Ionic fluids: Journal of Physical Chemitry, v. 88, p. 2689–2697.

Pitzer, K. S., Bischoff, J. L., and Rosebauer, R. J., 1987, Critical behavior of dilute NaCl in H_2O: Chemical Physics Letters, v. 134, p. 60–63.

Pitzer K. S., and Li, Y.-g, 1984, Critical phenomena and thermodynamics of dilute aqueous sodium chloride to 823 K: Proceedings of the National Academy of Sciences, v. 81, p. 1268–1271.

Pitzer, K. S., and Pabalan, R. T., 1986, Thermodynamics of NaCl in steam: Geochimica et Cosmo-chimica Acta, v. 50, p. 1445–1454.

Pitzer, K. S., Peiper, J. C., and Busey, R. H., 1984, Thermodynamic properties of aqueous sodium chloride solutions: Journal of Physical Chemistry Reference Data, v. 13, p. 1–102.

Potter, R. W. II, Babcock, R. S., and Brown, D. L., 1977, A new method for determining the solubility of salts in aqueous solutions at elevated temperatures: Journal of Research of the United States Geological Survey, v. 5, p. 389–395.

Rosenbauer, R., and Bischoff, J. L., 1987, Pressure-composition relations for coexisting gases and liquids and the critical points in the system NaCl-H_2O at 450, 475, and 500°C: Geochimica et Cosmochimica Acta, v. 51, p. 2349–2354.

Rowlinson, J. S., and Swinton, F. L., 1982, Liquids and Liquid Mixtures, 3d ed.: London, Butterworths, 328 p.

Schröer, E., 1927, Untersuchungen uber den kristischen Zustand: Zeitschrift fur Physik und Chemie, v. 129, p. 79–110.

Sourirajan, S., and Kennedy, G. C., 1962, The system NaCl-H_2O at elevated temperatures and pressures: American Journal of Science, v. 260, p. 115–242.

Tanger, J. C., and Pitzer, K. S., in press, Thermodynamics of NaCl-H_2O: a new equation of state for the near-critical region and comparisons with other equations for adjoining regions: Geochimica et Cosmochimica Acta.

Urusova, M. A., 1974, Phase equilibria in the sodium-hydroxide-water and sodium chloride-water systems at 350–550°C: Russian Journal of Inorganic Chemistry, v. 19, p. 450–454 (English translation).

———— 1975, Volume properties of aqueous solutions of sodium chloride at elevated temperatures and pressures: Russian Journal of Inorganic Chemistry, v. 20, p. 1717–1721 (English translation).

Wood, S. A., Crerar, D. A., Brantley, S. L., and Borcsik, M., 1984, Mean molal stoichiometric activity coefficients of alkali halides and related electrolytes in hydrothermal solutions: American Journal of Science, v. 284, p. 668–705.